Chemical Science

ROYAL SOCIETY OF CHEMISTRY

REVIEW

View Article Online
View Journal | View Issue

Cite this: *Chem. Sci.*, 2026, **17**, 6324

Recent advances in small-molecule fluorescent probes for simultaneous dual detection of HClO/ClO$^-$ and analytes/microenvironment

Yongqing Zhou,*[a] Mei Yan,[a] Hosoowi Lee[b] and Juyoung Yoon *[bc]

Hypochlorous acid/hypochlorite (HClO/ClO$^-$) is one of the most crucial reactive oxygen species that exert effective antibacterial effects in living organisms. Real-time monitoring of HOCl/ClO$^-$ changes in the local regions will help to further reveal its biological functions. However, the alterations of HClO/ClO$^-$ and other analytes/microenvironment often fluctuate simultaneously in the occurrence and progress of certain diseases. That is to say, a large number of pathological processes are controlled by various biological species and microenvironment. Therefore, exploring the interactive relationship and co-regulation mechanism between HClO/ClO$^-$ and analytes/microenvironment is vital. Fluorescence imaging techniques have been broadly applied in detecting HClO/ClO$^-$ and analytes/microenvironment in biological systems due to their outstanding performance, including non-invasiveness, *in situ* capability, and high spatial–temporal resolution. Fluorescent probes have been considered as one of the most efficient instruments for studying molecular events. Herein, this review offers a comprehensive statement of dual-responsive small-molecule fluorescent probes for simultaneous monitoring of HClO/ClO$^-$ and analytes/microenvironment. Furthermore, the levels, distributions and relationship of HClO/OCl$^-$ and analytes were revealed in depth, especially latent functions in numerous diseases. In particular, this review may offer valuable references for the preparation and application of simultaneous dual-detection fluorescent probes in the future.

Received 12th November 2025
Accepted 19th February 2026

DOI: 10.1039/d5sc08843g

rsc.li/chemical-science

1. Introduction

Hypochlorous acid/hypochlorite (HClO/ClO$^-$) is one of the most crucial reactive oxygen species (ROSs) and plays a crucial role in multitudinous physiological and pathological processes.[1] ClO$^-$ is in equilibrium with hypochlorous acid (HClO, pK_a = 7.53) under physiological conditions.[2] Generally speaking, the average generation rate of HClO has been determined to be 0.47 nM min^{-1} in 10^6 cells. Within the concentration range, HClO/ClO$^-$ participates in the immune defense system, and is capable of eliminating invading bacteria and pathogens.[3] However, the increased HClO/ClO$^-$ levels are closely associated with a variety of symptoms and diseases.[4–6] Meantime, numerous studies have discovered that the occurrence and development of certain diseases are related to variations of HClO/ClO$^-$ and other analytes/microenvironment.[7–10] That is to say, the interrelationships and synergistic regulation of HClO/ClO$^-$ and other analytes/microenvironment are involved in some diseases. In particular, a large number of physiological and pathological processes are controlled by various biological species and microenvironment parameters. Thus, simultaneously and accurately detecting HClO/ClO$^-$ and analytes/microenvironment is crucial for exploring their underlying roles and mechanisms.

In comparison to other detection methods, mainly including electrochemical methods and spectrophotometry, fluorescence imaging technology boasts numerous detection advantages, such as non-invasiveness, *in situ* capability, high sensitivity and temporal and spatial resolution. Up to now, small-molecule fluorescent probes have served as decent tools for studying variations of reactive species and the microenvironment.[11–34] In particular, dual-channel fluorescent probes have also been extensively constructed and applied in disease diagnosis.[35–44] Meanwhile, amounts of small-molecule fluorescent probes for concurrently detecting HClO/ClO$^-$ and analytes/microenvironment were consecutively designed. Furthermore, the dynamic variations and collaborative mechanism of HClO/ClO$^-$ and analytes/microenvironment were drastically disclosed *via* these fluorescent probes. Therefore, the single-structure and double-response fluorescent probes were decent choices for successfully detecting HClO/ClO$^-$ and analytes/microenvironment in cells and *in vivo*.

[a]*School of Chemistry and Chemical Engineering, University of Jinan, Jinan, 250022, People's Republic of China. E-mail: chm_zhouyq@ujn.edu.cn*

[b]*Department of Chemistry and Nanoscience, Ewha Womans University, Seoul 03760, Korea. E-mail: jyoon@ewha.ac.kr*

[c]*Graduate Program in Innovative Biomaterials Convergence, Ewha Womans University, Seoul 03760, Korea*

Upon to now, dual-detection small-molecule fluorescent probes have usually contained two fluorescent reporters and two recognition units. After the sensing moieties reacted with different reactive molecules, these fluorescent probes emitted differentiable emission peaks, thereby achieving the purpose of distinction and detection of diverse analytes (Fig. 1a). Employing this sensing principle, many researchers have successfully worked on using a single-structure fluorescent probe to distinguishably image HClO/ClO^- and analytes ($ONOO^-$, NO, H_2O_2, $^{\bullet}OH$, SO_2, H_2S, Cys, ATP, NQO1, β-gal). In addition, reactive molecule variations were often accompanied by alterations in the microenvironment (viscosity, polarity and pH). In view of this reason, the joint fluctuations of HClO/ClO^- and the microenvironment tend to cause fluctuations in the occurrence and development of many diseases. Let's explain this using viscosity as an example. As depicted in Fig. 1b, in a high-viscosity medium, the single bond rotation was restricted in the probe structure, triggering intense fluorescence, realizing the detection of viscosity. Analogously, upon responding with HClO/ClO^-, the identifying group was degraded, generating free fluorophore, accompanied by intense fluorescence signals. In this work, we summarized the recent development of dual-channel small-molecule fluorescent probes for the coinstantaneous monitoring of HClO/ClO^- and analytes/microenvironment. This review classifies the molecular structures, responsive mechanisms, optical properties, and biological imaging of these small-molecule fluorescent probes (Table 1). Furthermore, the prospects, challenges and opportunities of this meaningful topic are also introduced, providing deeper insights for the subsequent construction of novel multifunctional fluorescent probes. Additionally, to better assist researchers in understanding the significance of optical properties, we present reported probes that simultaneously detect reactive molecules/microenvironment in living systems.

2. Dual-detection small-molecular fluorescent probes

2.1 Detecting HClO/ClO^- and RNSs

Reactive nitrogen species (RNSs) participate in cellular signal transduction in various physiological and pathological processes. Among them, superfluous peroxynitrite ($ONOO^-$) has been proven to damage various biomolecules, such as thiols, lipids, proteins, carbohydrates, DNA, *etc.*, because it promotes oxidation reactions. Due to the significance of HClO and RNSs in human health and diseases, the exploration of their biological functions has become an important research field. Thus, it is of great significance to explore their functions, interrelationships and cooperation mechanism in the occurrence and development of related diseases. For instance, Han's group proposed a molecular fluorescent probe (PTZ-H) with double recognition sites (Fig. 2), which could concurrently detect ClO^- and $ONOO^-$ in *in vitro* experiments.[45] The S atom in the coumarin containing phenothiazine was selected as the responsive unit for ClO^-, while the boronate ester was used as the sensor for $ONOO^-$. In *in vitro* experiments, the probe itself emitted red fluorescence at 640 nm. Nevertheless, upon responding to ClO^- and $ONOO^-$, PTZ-H was converted into two products along with green fluorescence at 520 nm and blue fluorescence at 450 nm (Fig. 3). Confocal fluorescence imaging experiments showed that PTZ-H distinguishably sensed ClO^- and $ONOO^-$ variations in live RAW 264.7 cells and zebrafish through different channels. As a result, PTZ-H was successfully enabled to explain the correlation between ClO^- and $ONOO^-$ under complex environments.

Yang's group reported a small-molecule fluorescent probe (CB2-H) for the recognition of HClO and $ONOO^-$ under a complex environment.[46] This molecular structure was composed of a coumarin and a benzopyrylium *via* a double

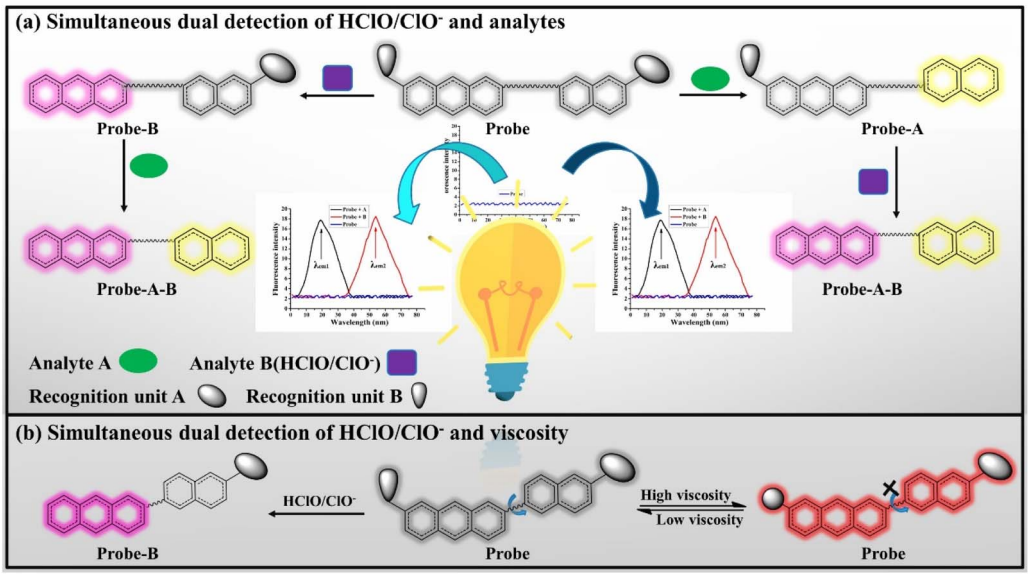

Fig. 1 Design strategy of small-molecule fluorescent probes for simultaneous dual detection of HClO/ClO^- and analytes (a)/viscosity (b).

Table 1 Optical performance and applications of fluorescent probes for simultaneous dual detection of HClO/ClO^- and analytes/microenvironment

Probe	Analytes	Excitation/nm	Emission/nm	Response mode	Detection limit	Applications	Ref.
PTZ-H	ClO^-	440	520/640	Ratiometric	17 nM	In cells, mouse liver slices, hippocampal slices	45
	$ONOO^-$	400	450/640	Ratiometric	About 21 nM		
CB2-H	HClO	400	468	Turn-on	35 nM	In cells, zebrafish	46
	$ONOO^-$	620	669	Turn-on	8.0 nM		
RhNp-ClO-ONOO	HClO	420	574	Turn-on	25.3 nM	In cells and rat model	47
	$ONOO^-$	420	518	Turn-on	12.4 nM		
DURC	HClO	400	464	Turn-on	58.6 nM	In cells	48
	$ONOO^-$	540	577	Turn-on	89.3 nM		
QBN	HClO	365	464	Turn-on	0.11 ± 0.03 μM	In cells	49
	NO	365	512	Turn-on	25.7 ± 3.4 nM		
FHZ	HClO	410	486	Turn-on	—	In cells and zebrafish	50
	$^{\bullet}OH$	490	520	Turn-on	—		
HR-SN	ClO^-	371	460	Turn-on	25.6 nM	In cells and zebrafish	51
	$^{\bullet}OH$	500	653	Turn-on	46.2 nM		
CSU1	HClO	376/440	520/640	Ratiometric	13 nM	In cells	52
	H_2O_2	376	409/640	Ratiometric	15 nM		
Probe 1	HClO	440	500/605	Ratiometric	0.064 μM	In cells, zebrafish, mice	53
	H_2O_2	360	450/605	Ratiometric	0.29 μM		
Geisha-1	ClO^-	400	452	Turn-on	28.2 nM	In cells and mouse liver tissues	54
	H_2O_2	450	550	Turn-on	64.6 nM		
FDOCl-N-Na	HClO	620	670	Turn-on	14.5 nmol L^{-1}	In cells, *Caenorhabditis elegans*	55
	H_2O_2	460	548	Turn-on	1.77 nmol L^{-1}		
PTZ-H–H	HClO	400	501	Turn-on	16.8 nM	In cells	56
	H_2O_2	470	685	Turn-on	386 nM		
MB-NAP	HClO	610	690	Turn-on	2.15 μM	In cells and mice with AKI	57
	Cys	450	560	Turn-on	1.61 μM		
HP	HClO	660	685	Turn-on	0.098 μmol L^{-1}	In cells, mouse model of peritonitis	58
	Cys	450	495	Turn-on	0.079 μmol L^{-1}		
Lyso-HA-HS	HClO	550	580	Turn-on	7.3×10^{-8} M	In cells	59
	H_2S	380	448	Turn-on	3.4×10^{-7} M		
RPC-1	HClO	545	580	Turn-on	19.8 nM	In cells and rat liver slices	60
	H_2S	360	445	Turn-on	192.1 nM		
Han-HClO–H_2S	HClO	400	450/640	Ratiometric	17 nM	In cells	61
	H_2S	440	520/640	Ratiometric	26 nM		
MB-NAP-N_3	HClO	620	686	Turn-on	0.032 μM	In cells, zebrafish	62
	H_2S	400	530	Turn-on	0.41 μM		
NACou	HClO	330	415	Turn-on	27.8 nM	In cells, actual samples, zebrafish, mice	63
	H_2S	440	539	Turn-on	34.4 nM		
MB-N-NAP	HClO	620	690	Turn-on	2.74 μM	In cells	64
	H_2S	450	533	Turn-on	0.535 μM		
MB-HS	HClO	620	689	Turn-on	0.26 μM	In cells	65
	H_2S	470	586	Turn-on	0.30 μM		
MTRN	HClO	530	616	Turn-on	3.39 nM	In cells	66
	H_2S	380	488	Turn-on	0.13 μM		
Probe CP	HClO	440	529/600	Ratiometric	0.0506 μM	In cells and alcoholic liver injury in mice	67
	H_2S	320	450/600	Ratiometric	1.7292 μM		
CyNa-N_3	HClO	660	775	Turn-on	0.17 μM	In cells	68
	H_2S	450	556	Turn-on	0.15 μM		
MPA-DNP	ClO^-	400	540	Turn-on	8.74 nM	In cells and mice	69
	H_2S	420	625	Turn-on	290.35 nM		
HBS-DNP	HClO	380	510	Turn-on	0.13 μM	In cells	70
	H_2S	380	598	Turn-on	0.69 μM		
HCy-SO_2–HClO	HClO	480	575	Turn-on	19.7 nM	In cells, zebrafish and mice	71
	SO_2	370	450	Turn-on	46.8 nM		
PBC1	HClO	380	485	Turn-on	13.0 nM	In cells, zebrafish	72
	SO_2	380	610	Turn-on	7.0 nM		
D-P	HClO	410	550	Turn-on	14 nM	In cells, zebrafish	73
	SO_2	415	486	Turn-on	0.9 nM		
RPT	HClO	450	510	Turn-on	0.65 μM	In cells, water, food	74
	SO_2	450	595	Turn-on	0.33 μM		
PTBI	HClO	456	590	Turn-on	45.8 nM	In cells and zebrafish	75
	SO_2	325	475	Turn-on	53.2 nM		

Table 1 (*Contd.*)

Probe	Analytes	Excitation/nm	Emission/nm	Response mode	Detection limit	Applications	Ref.
BEDB	ClO^-	540	575	Turn-on	401.5 nM	In real samples, cells, zebrafish	76
	SO_2	383	467	Turn-on	41.2 nM		
$P_{β\text{-gal–HClO}}$	HClO	630	700	Turn-on	0.15 μM	In cells	77
	β-Gal	450	560	Turn-on	0.36 mU mL^{-1}		
Probe NH	HOCl	400	517/643	Ratiometric	0.0065 μM	In cells	78
	NQO1	400	483/643	Ratiometric	0.0153 μg mL^{-1}		
RATP–NClO	ClO^-	420	534	Turn-on	0.10 μM	In cells and MASH mouse model	79
	ATP	520	587	Turn-on	4.13 μM		
RhFNMB	HClO	620	688	Turn-on	0.129 μM	In cells and mice with rheumatoid arthritis	80
	ATP	520	586	Turn-on	3.3 μM		
Probe 1	ClO^-	630	685	Turn-on	3.17 μM	In cells	81
	ATP	460	590	Turn-on	340 μM		
A-H	HClO	650	685	Turn-on	0.025 μM	In cells	82
	ATP	531	556	Turn-on	80 nM		
1	HClO	550	670/705	Turn-on	15.3 nM	In cells	83
	Zn^{2+}	482	653	Turn-on	1.39 mM		
LL3	ClO^-	430		Turn-on	1.46 μM	In cells	84
	Cu^{2+}	430	475/493	Turn-on	0.19 μM		
FP	ClO^-	330	376	Turn-on	35.9 nM	In cells	85
	Fe^{3+}	510	582	Turn-on	49.1 nM		
dfBDP	HClO	500	575	Turn-on	33.9 nM	In cells and mice	86
	F^-	780	940	Turn-on	316.2 nM		
NS	HClO	430	548	Turn-on	11.4 nM	In cells, soil sample, *Pseudomonas aeruginosa*	87
	N_2H_4	340	448	Turn-on	48 nM		
PTZ-BA	HClO	405	490/680	Ratiometric	11 nM	In cells and zebrafish	88
	N_2H_4	405	525/680	Ratiometric	15 nM		
PTMQ	ClO^-	460	577	Turn-on	58 nM	In cells	89
	N_2H_4	360	500	Turn-on	89 nM		
PI	HClO	375	490	Turn-on	41 nM	In cells, zebrafish, and *Arabidopsis thaliana*	90
	N_2H_4	375	520	Turn-on	23 nM		
Lyso-VH	HClO	400	500	Turn-on	73 nM	In cells and mice with acute lung injury	91
	Viscosity	475	580	Turn-on	—		
AS-CN	HClO	395	593	Turn-on	12 nM	In cells and atherosclerosis mice	92
	Viscosity	460	710	Turn-on	—		
M-2	HClO	530	562	Turn-on	0.072 nM	In cells, atherosclerosis mouse models	93
	Viscosity	530	656	Turn-on	—		
HBTN	HClO	405	530/680	Ratiometric	24.5 nM	In cells, zebrafish	94
	Viscosity	405	680	Turn-on	—		
TTD	ClO^-	371	460	Turn-on	33 nM	In cells	95
	Viscosity	470	600	Turn-on	—		
JXR	HClO	400	470/594	Ratiometric	95.7 nM	In cells, zebrafish	96
	Viscosity	400	594	Turn-on	—		
NS	HClO	465	540/600	Ratiometric	116 nM	In cells	97
	Viscosity	425	530	Turn-on	—		
Probe 1	ClO^-	380	493/628	Ratiometric	0.082 μM	In cells and zebrafish	98
	Viscosity	500	630	Turn-on	—		
PBI	ClO^-	400	577	Turn-on	192.3 nM	In cell and zebrafish	99
	Viscosity	400	459	Turn-on	—		
TPP-AN	ClO^-	370	414/620	Turn-on	65.1 nM	In cells	100
	Viscosity	370	416/600	Ratiometric	—		
CTPA	HClO	410	456	Turn-on	11.9 nM	In cells	101
	Polarity	440	605	Turn-on	—		
BA-PTZ	HClO	350	500	Turn-on	37 nM	In cells	102
	Polarity	475	675	Turn-on	—		
RN-HP	HClO	545	577	Turn-on	59.8 nM	In cells and actual samples	103
	pH	360	460	Turn-on	—		

bond. The spirocyclic structure of CB2-H displayed dim NIR emission because of the interruption of its extensive π conjugation structure. Additionally, the fluorescence of coumarin was significantly quenched, because of the intramolecular photoinduced electron transfer (PET) mechanism. $ONOO^-$ could oxidize the hydrazide group in the probe, and then obtained the

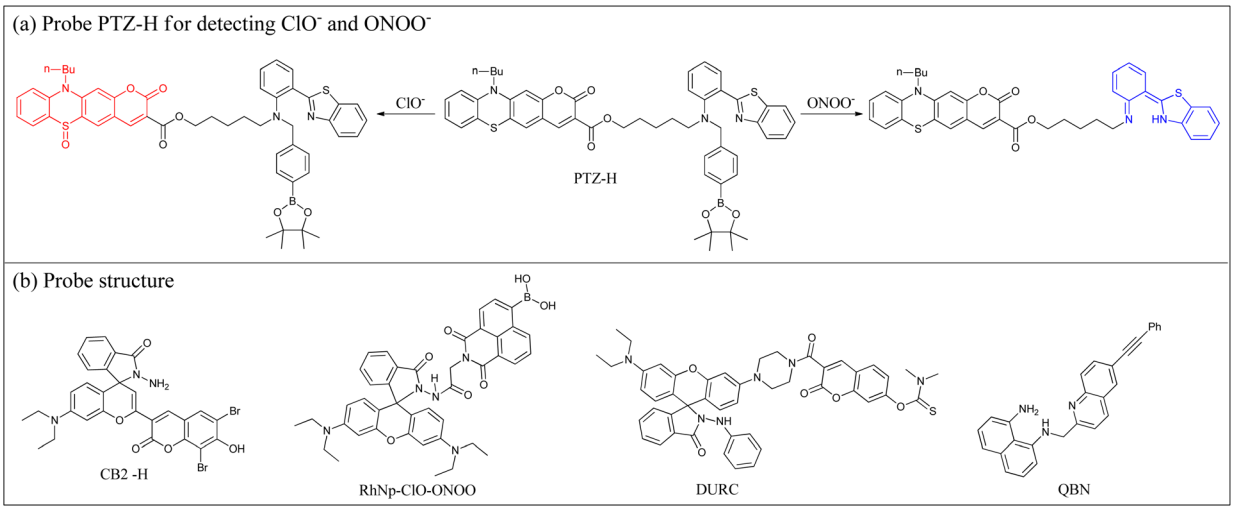

Fig. 2 (a) Sensing mechanism of probe PTZ-H and (b) molecular structures of fluorescent probes.

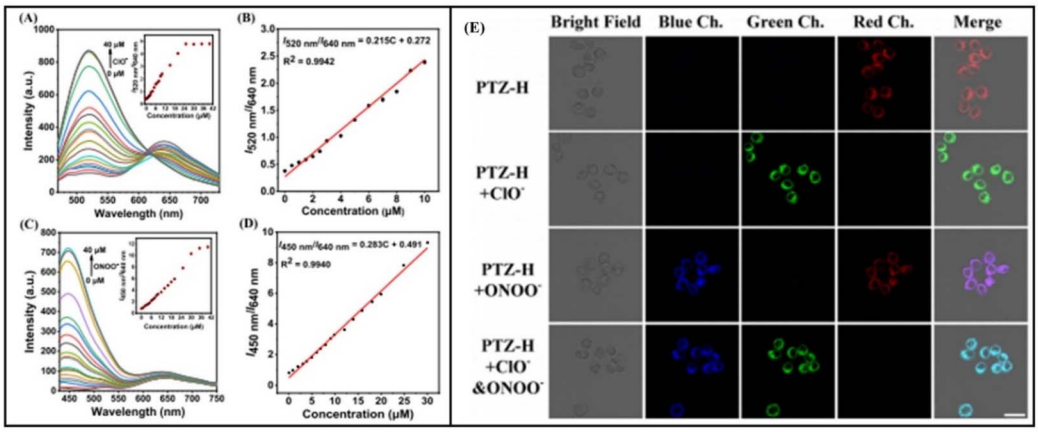

Fig. 3 Optical properties and intracellular fluorescence imaging of fluorescent probe PTZ-H. (A and C) Fluorescence spectra for PTZ-H with different concentrations of ClO^- and $ONOO^-$. (B and D) Linear relation between ratiometric fluorescence intensity and ClO^- and $ONOO^-$. (E) Fluorescence imaging of PTZ-H in cells. This figure has been reproduced from ref. 45 with permission from American Chemical Society, copyright 2022.

new product with opening form, accompanied by stronger NIR emission. In contrast, HClO attacked on the benzopyran moiety, and then generated the chlorinated product, thereby resulted in an open-ring fluorescence response. The CB2-H simultaneously monitored the endogenous HClO and $ONOO^-$ production in living cells and zebrafish under various stimuli. The CB2-H was used for dual-channel fluorescence imaging of endogenous HClO and $ONOO^-$ variations in living cells and zebrafish under stimulation conditions. In short, the CB2-H may serve as a useful tool for comprehending the distribution and correlations of HClO and $ONOO^-$ in biological systems.

Zhou's team rationally utilized the rhodamine B and 4-hydroxynaphthalimide to construct a novel dual-responsive fluorescent sensor (RhNp-ClO-ONOO).[47] In the design, the bis-hydrazide and boronic acid severally served as an acknowledged HClO-responsive group and a $ONOO^-$-responsive moiety. In *in vitro* experiments, RhNp-ClO-ONOO resoundingly distinguished $ONOO^-$ and HClO through different fluorescence signals. Furthermore, RhNp-ClO-ONOO quickly sensed HClO (approximately 60 s) and $ONOO^-$ (about 20 s) in buffer solution. Additionally, RhNp-ClO-ONOO could successfully image endogenous HClO and $ONOO^-$ in cells, inflammatory tissues and mouse models. Thus, RhNp-ClO-ONOO was used for biological imaging HClO and $ONOO^-$ in future work, eventually achieving early diagnosis of mediated inflammatory diseases.

Tang's team prepared a new fluorescent probe (DURC) by pairing two fluorescent compounds (7-hydroxycoumarin and rhodamine) with the recognition groups (dimethylthiocarbamate and phenylhydrazine).[48] After reaction with HClO or $ONOO^-$, the dimethylthiocarbamate or phenylhydrazine unit was discerned, and then free fluorophore was liberated, accompanied by dazzling fluorescence (at 464 nm and 577 nm). Employing this sensing mechanism, the DURC displayed impressive detection performance, including a lower

limit of detection and distinguishable detection. Subsequently, DURC was used for monitoring intracellular HClO and $ONOO^-$ influxes *via* diverse channels.

Wang's group used a quinoline and 1,8-diamino naphthalene derivatives as the fluorophore and reaction unit to prepare an "off–on" type fluorescent probe (QBN).[49] The probe itself displayed faint fluorescence in view of the existence of the PET process. The QBN reacted either with HClO or nitric oxide (NO), generating different products along with dazzling fluorescence at 464 nm and 512 nm, respectively. Through mass spectrometry analysis, the different products obtained by the reaction of QBN with HClO or NO could be identified, proving different response mechanisms. The confocal fluorescence imaging evidence demonstrated that feasibility of QBN simultaneously detecting these two substances (HClO and NO) was quite popular. Finally, the direct and intuitive method for simultaneous imaging of endogenous HClO and NO contributed to the observed overexpression of HClO and the consumption of NO in RAW 264.7 cells.

By employing various recognition groups, the researchers have developed a series of high performing dual-responsive fluorescent probes. Moreover, the researchers used these molecular probes as detection tools to achieve visual imaging of the changes in $HClO/ClO^-$ and $ONOO^-$ in different disease models, such as inflammatory rat models. As the experimental results had shown, the changes of HClO were correlated with the presence of $ONOO^-$ in inflammatory rat models. Additionally, using QBN, overexpression of HClO and the consumption of NO in RAW 264.7 cells were directly visualized. Profoundly, these molecular fluorescent probes displayed distinguishable fluorescence spectra in the presence of $HClO/ClO^-$ or $ONOO^-$. The successful development of these detection tools contributed to the elucidation of the roles of $HClO/ClO^-$ and $ONOO^-$ in the pathological mechanism.

2.2 Detecting $HClO/ClO^-$ and ROSs

Apart from HClO, there are also numerous other ROSs present in living organisms, mainly including the hydroxyl radical ($^{\cdot}OH$) and hydrogen peroxide (H_2O_2). Although ROSs produced in normal cellular environments are crucial for life activity, excessively generated ROS can trigger intracellular oxidative stress by oxidizing biomolecules (such as proteins and DNA), leading to cell death, eventually resulted in multitudinous diseases. H_2O_2, a vital product of oxygen metabolism, is tightly related to diverse human diseases. Under the condition of a single electron metal ion (such as Fe^{2+}), H_2O_2 will be converted into $^{\cdot}OH$, thereby initiating the Ferret reaction. To conduct a more in-depth analysis of HClO and $^{\cdot}OH/H_2O_2$ variations and to clarify their roles within living organisms, for example, Zhang's team dexterously synthesized a new molecular fluorescent probe (FHZ) using a fluorescein skeleton.[50] This FHZ simultaneously distinguished and analyzed $^{\cdot}OH$ and HClO variations in living organisms. The FHZ was legitimately designed by attaching an additional five-membered heterocyclic ring and a lateral triethylene glycol chain to the fluorescein (Fig. 4). The reactivity of the FHZ with $^{\cdot}OH$ and HClO, respectively, exhibited blue and green fluorescence, thereby providing a basis for real-time identification. The FHZ could monitor ROS in real time in various organs, which may serve as a practical sensor for investigating other ROS variations.

A novel dual-detection fluorescent probe (HR-SN) was synthesized for the rapid detection of $^{\cdot}OH$ and HClO.[51] This

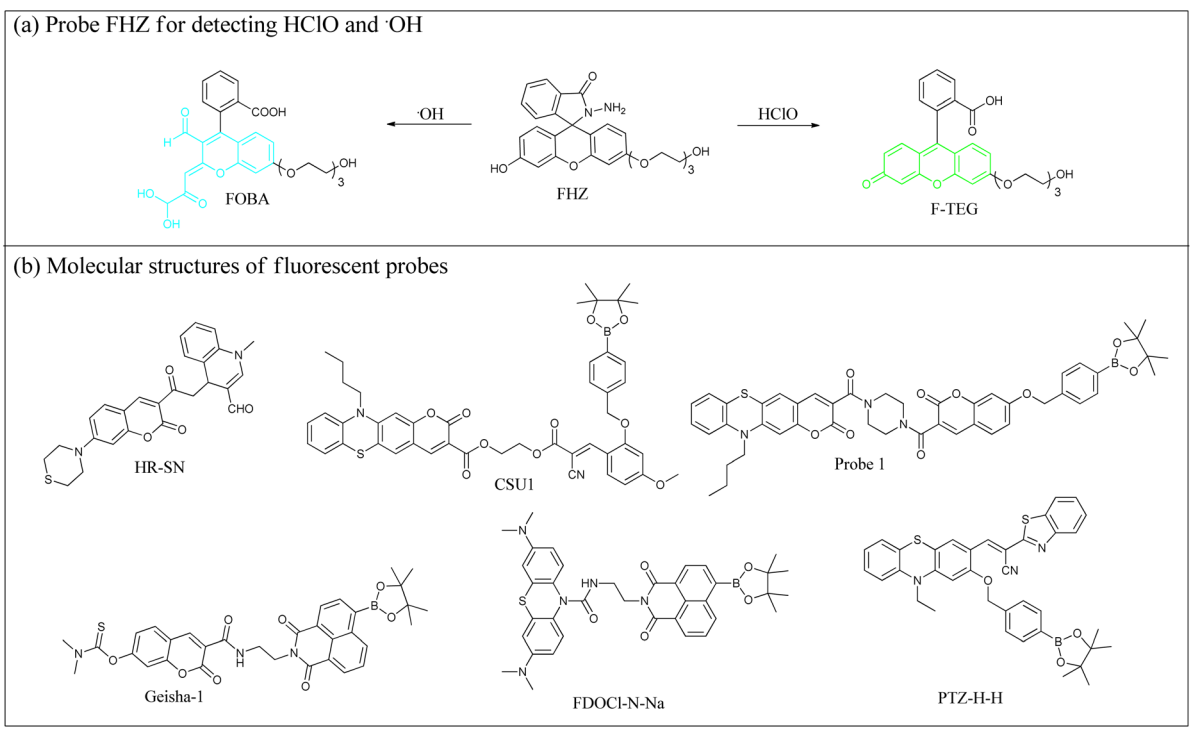

Fig. 4 (a) Sensing mechanism of FHZ and (b) molecular structures of fluorescent probes.

coumarin–quinoline hybrid structure, thiomorpholine and an acetyl group were severally regarded as fluorophores, the recognition sites for HClO and ˙OH. The HR-SN exhibited a significant fluorescence enhancement upon expose to ˙OH or HClO, featuring a notable Stokes shift, rapid response and high sensitivity. The biological imaging results confirmed that this HR-SN was suitable for monitoring ˙OH and HClO in cells and zebrafish. Therein, this study provided valuable references for creating molecular probes for detecting two ROSs in tanglesome environments.

Song's team intelligently created a new ratiometric fluorescent probe (CSU1) that could concurrently monitor HClO and H_2O_2.[52] A coumarin derivate containing phenothiazine served as the chromophore and sensor for HClO, and another coumarin derivate containing boronate ester acted as the recognition unit for H_2O_2 (Fig. 5). The CSU1 exhibited outstanding characteristics, such as high sensitivity. The confocal fluorescent imaging experiments proved that CSU1 had the capability of selectively and sensitively detecting HClO and H_2O_2, accompanied by differentiable fluorescence channels. Moreover, this CSU1 successfully imaged H_2O_2 and HClO in living cells through different fluorescence signals. The work demonstrated that this CSU1 may serve as a powerful tool for inspecting the interaction between HClO and H_2O_2 under oxidative stress.

Liu's group developed a new dual-sensitive fluorescent probe (1) for simultaneously identifying HClO and H_2O_2.[53] This probe 1 was designed by utilizing coumarin containing phenothiazine (the HClO sensing unit) and boric acid ester (the H_2O_2 identifying unit). Experimental results certified that this probe 1 independently imaged HClO and H_2O_2 in organisms. Importantly, probe 1 monitored HClO and H_2O_2 fluctuations in cells, zebrafish, and mice with alcoholic liver injury.

A novel dual-channel fluorescent probe (Geisha-1) was reported for the identification of ClO^- and H_2O_2.[54] The probe's structure was prepared by reasonably implanting *N*,*N*-dimethylthiocarbamate and boronate ester *via* introducing the fluorescence resonance energy transfer (FRET) process. Geisha-1 exhibited excellent sensitivity with a lower detection limit (28.2 nM for ClO^- and 64.6 nM for H_2O_2) in *in vitro* experiments. Subsequently, Geisha-1 was consecutively used for imaging ClO^- and H_2O_2 within cells and tissues, demonstrating its potential application for diagnosis of certain diseases.

A difunctional fluorescent probe (FDOCl-N-Na) was fabricated for sensing H_2O_2 and HClO variations.[55] FDOCl-N-Na exhibited a prominent response ability to H_2O_2 and HClO, showing green and red fluorescence. Confocal fluorescent imaging tests demonstrated that FDOCl-N-Na was capable of monitoring endogenous H_2O_2 and HClO fluctuations under stimulation by various inducers. Additionally, FDOCl-N-Na possessed the capability of tracking the fluctuations of H_2O_2 and HClO in *Caenorhabditis elegans*. In short, FDOCl-N-Na had the capability of detecting H_2O_2 and HClO within cells, and could be considered as an effective sensor for identifying cancer.

Song's group introduced a dual-site fluorescent probe (PTZ-H–H), which separately and continuously detected intracellular H_2O_2 and HClO.[56] PTZ-H–H displayed selective and sensitive detection toward H_2O_2 and HClO in the buffer solution. The reactive systems emitted red or green fluorescence upon reaction with H_2O_2 or HClO. PTZ-H–H was successfully applied in real-time imaging of H_2O_2 and HClO. This PTZ-H–H could visualize the dynamic interactions of two ROSs under complex systems.

Summing up, among the molecular probe structures reported here, some of the fluorescent probes had simple designs but exhibited remarkable detection capabilities, such as FHZ. Meanwhile, these sensors enabled the simultaneous detection of HClO and other ROSs (mainly including H_2O_2 and ˙OH) *via* double independent channels. Furthermore, these probes were used for detecting two ROSs without spectral cross-interference in cells, zebrafish, tissue and mice. Utilizing these detection tools, the influxes and distributions of the two ROSs were triumphantly observed with the assistance of a fluorescence confocal microscope. Notably, these two ROSs changes showed consistency in certain pathological processes and diseases, such as alcoholic liver injury in mice. In particular, most of these sensors possessed the advantage of ratiometric detection for HClO/ClO^- and other ROSs (H_2O_2, ˙OH), carrying out quantitative detection of two ROSs. These detection tools were

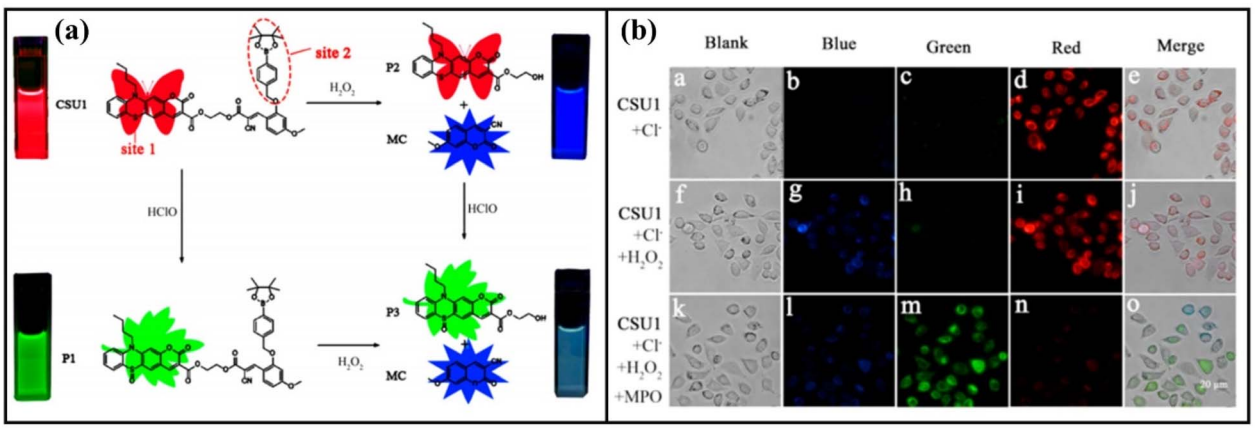

Fig. 5 (a) Recognition mechanism and (b) intracellular fluorescence imaging of fluorescent probe CSU1. This figure has been reproduced from ref. 52 with permission from American Chemical Society, copyright 2020.

helpful in establishing the relationship between ROSs concentrations and the degree of damage. Given that this is a benchmark, these tools were applied in early diagnosis and treatment of diseases.

2.3 Detecting HClO/ClO$^-$ and RSSs

Appropriate levels of ROSs and reactive sulfur species (RSSs) are involved in cell signal transduction, substance synthesis and metabolism, as well as other activities. Therein, cysteine (Cys), sulfur dioxide (SO_2), and hydrogen sulfide (H_2S) play crucial roles in maintaining the redox balance, regulating signal transduction. Their functions as antioxidants and free radical scavengers play a key role in some diseases. Some reports indicated that HClO/ClO$^-$ and RSSs are linked with normal physiological processes and major human diseases. Developing a precise and efficient method for measuring intracellular

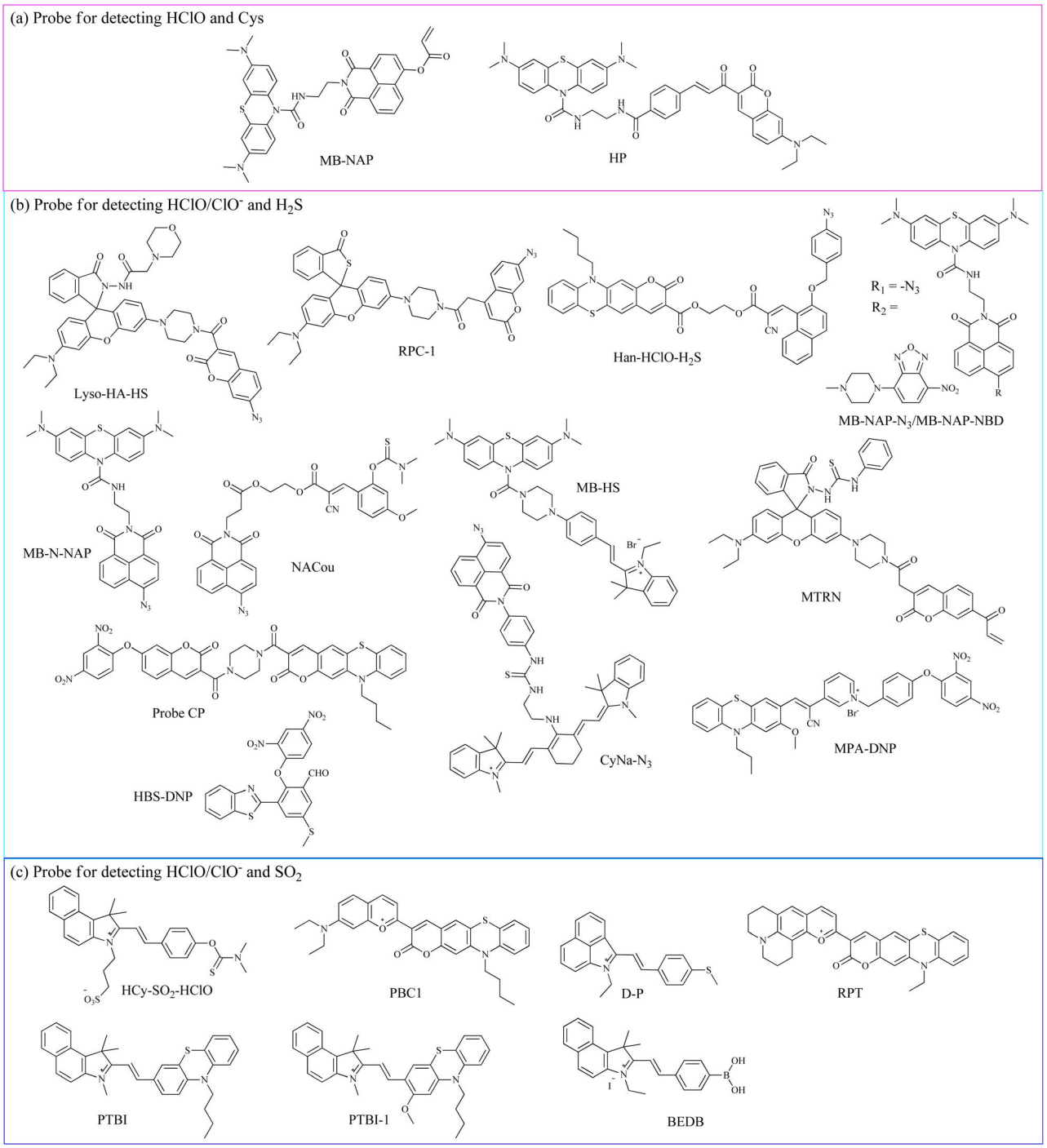

Fig. 6 Molecular structures of fluorescent probes. (a) Probes for detecting HClO and Cys. (b) Probes for detecting HClO/ClO$^-$ and H_2S. (c) Probes for detecting HClO/ClO$^-$ and SO_2.

HClO/ClO$^-$ and RSSs is of great significance for further research on their physiological functions and early disease diagnosis.

Wang's group created a novel dual-channel fluorescent probe (MB-NAP).[57] In this structure, the hydroxyl unit in the naphthalimide reacted with acryloyl chloride to form acrylate, which served as the recognition site for Cys (Fig. 6). Upon interaction with Cys, the Michael addition reaction occurred and generated the corresponding thiol, then released the naphthalimide moiety, ultimately resulting in enhanced fluorescence in the green channel. Therefore, MB-NAP simultaneously detected HClO and Cys *via* diverse fluorescence peaks. This MB-NAP exhibited distinct fluorescence variations through multiresponse signals, avoiding spectral interference. Subsequently, researchers successfully applied MB-NAP to monitor HClO and Cys levels in acute kidney injury (AKI) mice (Fig. 7). Moreover, the consequence showed that their concentrations in AKI mice were dramatically higher than those in the normal models. By simultaneously imaging HClO and Cys, their underlying roles in the process of AKI were successfully revealed using independent fluorescence channels.

Yin's group designed a dual-sensitive fluorescent probe (HP), which simultaneously sensed intracellular HClO and Cys concentrations.[58] In the probe design, ethylenediamine was used to connect coumarin and methylene blue. The emission peaks of solutions containing probe HP and Cys and HClO differed significantly, avoiding spectral overlap. Moreover, the α,β-unsaturated ketone and amide bond were severally recognized as reactive sites for Cys and HClO. After the HP recognized Cys or HClO, the green fluorescence of the reactive solution shifted to blue or red fluorescence, thereby achieving simultaneous and distinguishable detection of Cys and HClO. Using probe HP, researchers successfully discovered the variations in the redox state mediated by HClO and Cys in live cells under the oxygen–glucose deprivation/reperfusion (OGD/R) model. Moreover, the fluctuations of endogenous HClO in mice with peritonitis induced by lipopolysaccharide were monitored *via* employing this probe. In summary, this study developed a credible tactic for visualizing and analyzing ROSs/RSSs, which was helpful for designing other sensors.

Lin's group developed a molecular tool (Lyso-HA-HS) with two recognition groups, which simultaneously detected HClO and H_2S in lysosomes.[59] Upon treatment with HClO, Lyso-HA-HS emitted prominent fluorescence in the red channel, demonstrating excellent selectivity and sensitivity. Upon exposure to H_2S, Lyso-HA-HS showed significant emission in the blue channel. Using this convenient probe Lyso-HA-HS, researchers achieved the imaging of lysosomal HClO and H_2S fluxes through their respective channels. Therefore, Lyso-HA-HS may become a convenient tool for investigating the underlying relation between redox balance and lysosomal function.

Tang's group synthesized a novel two-photon fluorescent probe (RPC-1) for the identification of HClO and H_2S in biological systems.[60] The probe used 7-amino coumarin and rhodamine B as fluorescent reporters, and azide and thiolactone as recognition units. After reacting with HClO and H_2S, RPC-1 showed two emission bands at 445 nm and 580 nm, achieving distinguishable distinction (Fig. 8). Under various experimental environments, RPC-1 monitored the influxes of intracellular HClO and H_2S. Moreover, *in vivo* experiment evidence demonstrated that HClO could be a suitable sensor of drug-induced liver injury (DILI) for assessing clinical drug-induced liver injury, while H_2S participated in the detoxification effect of *N*-acetyl-L-cysteine (NAC), which contributed to studying the efficacy of detoxification agents, ultimately exploring their molecular mechanisms.

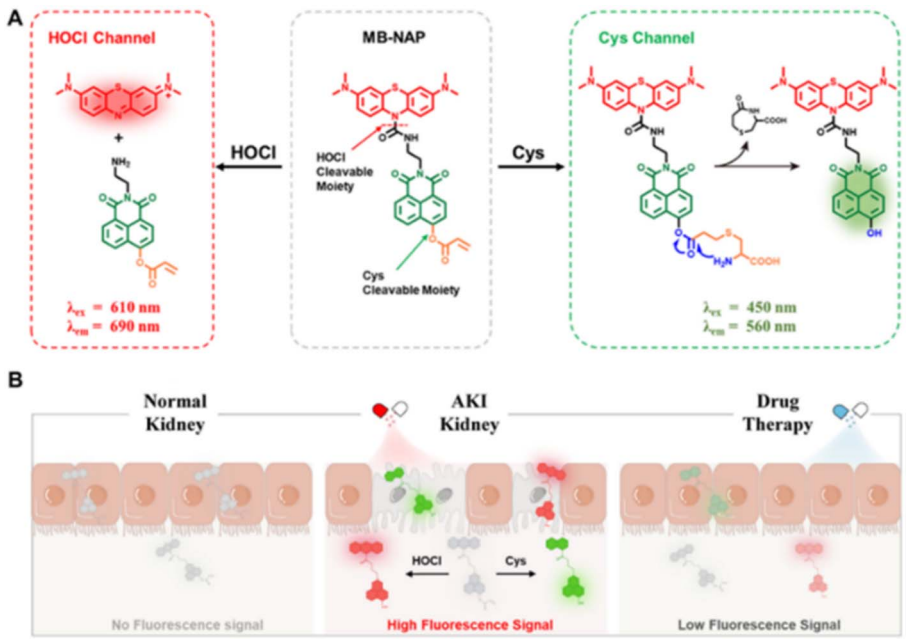

Fig. 7 (A) The reaction mechanism and (B) biological applications of the probe MB-NAP. This figure has been reproduced from ref. 57 with permission from American Chemical Society, copyright 2025.

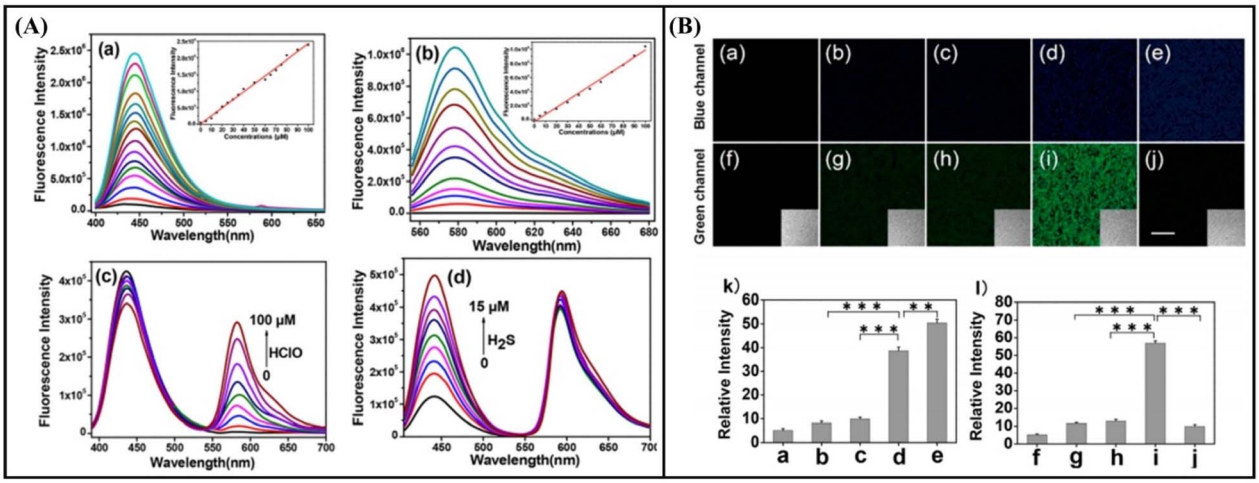

Fig. 8 (A) The optical properties of the probe RPC-1. (B) Fluorescence imaging of APAP-induced hepatotoxicity. This figure has been reproduced from ref. 60 with permission from American Chemical Society, copyright 2018.

Song's group presented a novel fluorescent probe (Han-HClO–H_2S) that simultaneously detected H_2S and HClO through a dual-ratiometric measurement method.[61] HClO enabled the oxidation of the phenothiazine in the probe structure, which triggered a distinct fluorescence change, realizing ratiometric detection. Upon exposure to H_2S, the azide group in the naphthalene was reduced and generated a coumarin with blue fluorescence, carrying out the ratiometric detection of H_2S. Moreover, Han-HClO–H_2S was successfully applied to image H_2S or HClO fluxes *via* multiresponse signals. The reasonable strategy employed in this study may potentially stimulate the development of dual-channel fluorescent probes for H_2S/HClO in complex systems.

Chen's group reported a molecular fluorescent probe (MB-NAP-N_3) employing the conjugated structure.[62] The probe itself featured methylene blue and naphthalimide. In this structure, the methylene blue served as the responding unit for HClO. The naphthalimide was selectively reduced by H_2S. Given the various recognition mechanisms, MB-NAP-N_3 severally sensed H_2S and HClO in the buffer solutions according to multiresponse signals. Due to its outstanding characteristics, MB-NAP-N_3 was successfully used for distinguishing endogenous and exogenous H_2S and HClO under different experimental conditions. To elucidate the interaction of H_2S and HClO in mice, the optimized construction strategy based on this MB-NAP-N_3 was continued to be applied in other fields. Therefore, the study is conducive to developing more powerful dual-response probes for monitoring other biomolecules.

Hou's group created a new dual-responsive fluorescent probe (NACou) for imaging HClO/H_2S.[63] The coumarin derivative (Cou-CN) and naphthalimide (NAP) were regarded as the fluorescent reporters in the probe design. *N*,*N*-Dimethylthiocarbamate served as the HClO-specific responsive moiety. Under the triggering of HClO, NACou underwent a nucleophilic and elimination reaction, obtaining the compound Cou-CN with strong blue fluorescence signals. Upon reacting with H_2S, the intramolecular charge transfer (ICT) mechanism of the NACou was recovered, which then generated intense green fluorescence signals. This NACou displayed high sensitivity and a low detection limit (HClO: 27.8 nM, H_2S: 34.4 nM). NACou possessed a remarkable fluorescence peak distance (124 nm), effectively minimizing the interference. NACou distinguished the variations in HClO/H_2S within cells and zebrafish, supporting an early warning for liver damage. Utilizing this identification principle, NACou was helpful in clarifying the complex relationships between HClO and H_2S during liver damage.

Zhang's group designed a dual-channel fluorescent probe (MB-N-NAP), which was used for simultaneously detecting H_2S and HClO in cancer.[64] The 4-azido-1,8-naphthalimide in the structure exhibited a specific response to H_2S, along with stronger green fluorescence, while the methylene blue derivative was responsive to HClO, generating red fluorescence. *In vitro* experiments indicated that MB-N-NAP possessed high sensitivity. Due to its excellent performance, MB-N-NAP was used for distinguishing endogenous H_2S and HClO in normal cells and cancer cells. Therein, MB-N-NAP may become an effective tool for analysis of cancer-related H_2S and HClO roles.

Ye's group synthesized a novel fluorescent probe (MB-HS) by combining methylene blue and indolium.[65] This MB-HS was capable of selectively detecting H_2S and HClO at different emission wavelengths. MB-HS exhibited several detection advantages toward H_2S and HClO in buffer solution. These key characteristics of MB-HS enabled the tracking of the endogenous H_2S and HClO fluctuations. Furthermore, the MB-HS had the capability of detecting H_2S and HClO variations in oxidative stress and ferroptosis. Therefore, this MB-HS may become an effective molecular sensor for discovery of the interactions of H_2S and HClO within living cells.

Pu's group designed a new molecular probe (MTRN) that specifically detected HClO and H_2S.[66] Coumarin and acrylate groups were used as the fluorophore and specific sensing unit for H_2S. The acrylate unit reacted with H_2S to form a product with the hydroxyl group, generating intense blue fluorescence,

on account of the generation of the ICT process. Meanwhile, a phenyl isothiocyanate in rhodamine served as a probe in the recognition of HClO. The MTRN possessed some detection superiorities, such as high sensitivity, low detection limit (HClO as low as 3.39 nM, H_2S as low as 0.13 μM), and fast response (within 2 min). Therefore, the MTRN was triumphantly used for imaging HClO and H_2S variations in HeLa cells.

This study reported a new dual-emission fluorescence sensor (CP) for the recognition of HClO and H_2S.[67] Upon reaction with HClO, the sulfur atom of the phenothiazine unit in the probe design underwent an oxidation reaction to form a sulfoxide, thereby causing the fluorescence to change from red to green, achieving a ratio-type detection. Meanwhile, 2,4-dinitroanisole in the probe design acted as the reactive group of H_2S. Subsequently, the probe CP was effectively applied in monitoring HClO and H_2S in cells, zebrafish models, and a mouse model of alcoholic liver injury. Through this distinct recognition principle, the probe CP achieved the distinction and detection of HClO and H_2S.

Pu's group constructed a novel dual-responsive fluorescent probe (CyNa-N_3) using cyanine and naphthalimide dyes.[68] This fluorescent probe exhibited higher sensitivity toward HClO and H_2S with a low detection limit utilizing red and green emission signals. Confocal fluorescence imaging results proved that CyNa-N_3 was used to distinguishably monitor HClO and H_2S in HeLa cells. The outstanding properties of CyNa-N_3 made it a potential sensor for the simultaneous detection of HClO and H_2S. In short, the research afforded a novel approach for preparing masses of dual-channel fluorescent probes.

Introducing phenothiazine and 2,4-dinitro-1-(*p*-tolyl)benzyl, Liu's team provided a small-molecule fluorescent tool (MPA-DNP) for distinguishing between detection of HClO and H_2S in biological systems.[69] Given its charming advantages, such as low detection limit, MPA-DNP had the capability of sensing HClO and H_2S in cells and inflammatory mice.

Introducing an aggregation-induced emission mechanism, Zhang's group constructed an activatable fluorescent probe (HBS-DNP), which specifically detected HClO and H_2S under complex systems.[70] In the design, an aldehyde group and 2,4-dinitrophenyl (DNP) ether for H_2S, and a methyl thioether group for HClO were implanted into benzothiazole dye. Upon treatment with HClO and H_2S, the reaction solution emitted remarkable red and green fluorescence, which was helpful for the distinction and detection of substances. Under stimulation of different reagents, such as lipopolysaccharide and phorbol myristate acetate, the intracellular fluorescence variations were clearly observed using a confocal fluorescence microscope.

Fu's group deftly reported a dual-responsive fluorescent probe (HCy-SO_2–HClO) for visualizing mitochondria HClO and SO_2 variations.[71] In the probe's structure, the introduction of the sulfonate group significantly enhanced the water solubility. In *in vitro* experiments, HCy-SO_2–HClO could quickly identify HClO and SO_2 within 10 s and 20 min, thereby achieving their fast detection. In co-localization experiments, HCy-SO_2–HClO prevailingly aggregated in the mitochondria. Utilizing the HCy-SO_2–HClO, HClO and SO_2 in heat shock-treated cells and mouse models were successfully distinguished for the first time, indicating that these two substances served as key biomarkers for the diagnosis of heat shock. Subsequently, employing this HCy-SO_2–HClO, researchers explored the relationship between redox homeostasis and heat shock by detecting HClO and SO_2 alterations. The work provided an effective strategy for the early prevention or treatment of heat shock-related diseases.

Introducing a benzopyrylium–coumarin hybrid structure, Song's group successfully developed a new dual-response fluorescent probe (PBC1) which simultaneously detected HClO and SO_2.[72] Given its low toxicity, PBC1 was also successfully used for imaging HClO and SO_2 in living systems. The PBC1 was able to differentiate between HClO and SO_2 by generating different fluorescence signals. Therefore, this PBC1 was used to investigate the functions and relation between HClO and SO_2 in various biological research studies.

Chen's group developed an intelligent fluorescent probe (D-P) with double-responsive sites.[73] The phenyl thioether moiety was considered as the sensing unit for HClO, and the double bond as the responding group for SO_2. This D-P possessed satisfactory detection superiorities toward HClO and SO_2 with different emission wavelengths, response time (6 s), and lower detection limit (14 nM). This D-P could also respond promptly to SO_2 within 40 s. Meanwhile, a lower detection limit of 0.9 nM was gained according to the corresponding formula. Furthermore, the D-P clearly discovered the variations of HClO and SO_2 under endoplasmic reticulum stress induced by DTT, hypoxia and ischemia stress. Finally, the D-P had the capability of assessing the dynamic balance of HClO and SO_2 in real time. Ultimately, the D-P was used as an early warning tool for monitoring oxidative stress and diseases.

A new dual-responsive fluorescent probe (RPT) for the detection of SO_2 and HClO was reasonably synthesized.[74] The RPT consisted of a pyrylium and a thiazine moiety. Upon treatment with SO_2, the entire π-conjugated structure was disrupted and then generated a new product along with red fluorescence at 595 nm. When HClO was presented in reactive solutions containing probe RPT, the S atom in the thiazine unit was oxidized and produced a sulfoxide unit, releasing a strong green fluorescence at 510 nm. This dual-responsive fluorescent probe showed a significant emission distance of about 85 nm, which effectually avoided fluorescent signal interference. Furthermore, the RPT was successfully used for monitoring intracellular SO_2 and HClO influxes *via* red and green channels. More importantly, the RPT had the capability of determining SO_2 and HClO concentrations in real water samples and food samples. This work proposed a new monitoring strategy based on dual-response fluorescent probes to monitor SO_2 and HClO variations.

To visualize the SO_2 and HClO levels, Zhou's team utilized phenothiazine and benzoindolium to synthesize two molecular fluorescent probes (PTBI and PTBI-1) through a C=C double bond.[75] Similarly, the S atom in the phenothiazine was specifically recognized by HClO, and triggered intense fluorescence in buffer solutions. The SO_2 underwent a nucleophilic addition reaction with the C=C double bond, and then generated a fluorescent product. Two products exhibited two well-separated emissions with a difference of 115 nm.

Impressively, the PTBI simultaneously monitored mitochondrial HClO and SO_2 variations under oxidative stress conditions. Afterwards, Zhang's group used phenylboronic acid to replace phenothiazine and developed a new type of fluorescent probe (BEDB) for monitoring their concentrations.[76] Employing the tool, the HClO and SO_2 fluctuations were monitored in cells and zebrafish *via* diverse emission channels.

The ROSs and RSSs within the cells jointly maintain the redox balance. Of course, when the HClO changed inside the cells, the levels of RSSs also fluctuated successively. Furthermore, the changes in HClO were negatively correlated with the changes in RSSs in some symptoms and diseases. The disruption of redox balance easily led to oxidative stress and caused certain diseases. Therefore, simultaneously detecting the ROS and RSS variations was helpful for monitoring the redox state. Presently, the successful development of these fluorescent probes offered a reference for the changes and distributions of dual-responsive HClO and other RSSs (Cys, SO_2, H_2S) in some diseases. For instance, NACou exhibited the capability of imaging HClO and H_2S variations in the process of liver damage. In addition, most of them could respond instantaneously to HClO, enabling *in situ* real-time detection. Importantly, these tools provided visual platforms for the diagnosis of diseases and the study of their mechanisms.

2.4 Detecting HClO/ClO^- and enzymes

Liu's group developed a dual-color fluorescent probe ($P_{\beta\text{-gal–HClO}}$).[77] In the probe's structure, 1,8-naphthalimide and methylene blue were selected as the double fluorescent reporters (Fig. 9). In *in vitro* experiments, the $P_{\beta\text{-gal–HClO}}$ could specifically respond to the two biomarkers (HClO and β-galactosidase, β-gal), generating non-interfering fluorescence signals. Confocal fluorescence imaging findings demonstrated that the $P_{\beta\text{-gal–HClO}}$ could detect HClO in the presence of other reactive species. Under the experimental environments, the intracellular fluorescence in both channels showed a significant enhancement. The expression levels of HClO in the foam cells related to atherosclerosis were completely revealed. Our research results provided a perfect example for designing a new dual-color fluorescent probe, which was expected to enhance our understanding of cell aging and age-related diseases.

Wang's group presented a dual-sensitive fluorescent probe (NH) for differentiating HClO and NAD(P)H:quinone oxidoreductase 1 (NQO1).[78] In the presence of HClO, the reacting solution containing NH changed from red to green color. Upon reaction of NQO1, fluorescence of reacting solutions changed from red to blue color. Moreover, this NH detected HClO and NQO1 variations in cell imaging experiments *via* introducing a dual-ratiometric method, which was applicable for evaluating the intracellular redox balance. This NH offered the possibility of investigating the correlation between HClO and NQO1 under redox homeostasis. This probe demonstrated great potential in analyzing the interrelationship between HClO and NQO1 in numerous processes.

Just as in the previous work, HClO and two enzymes (β-gal and NQO1) were indeed involved in certain symptom, such as cellular senescence. The research findings provided a good example for preparing dual-color fluorescent probes for deepening our understanding of cellular aging and age-related diseases. Thus, with this successful case, a new path was opened for future research on HClO and enzymes. Regrettably, the signaling pathways involving HClO in enzymatic activities have not been fully elucidated.

2.5 Detecting HClO/ClO^- and ATP

Adenosine-5′-triphosphate (ATP) is a crucial source of energy and is indispensable for various cellular activities, with its levels ranging from 1 to 10 mM. For example, the ATP concentrations decreased in the process of metabolic dysfunction-associated steatotic liver disease, due to the impaired mitochondrial function or disrupted metabolic pathways in liver cells. The decrease in ATP levels indicated that the liver was damaged, and the interaction between ATP and HClO levels was related to oxidative stress-mediated mitochondrial dysfunction and intracellular damage. Therefore, Lee's group prepared a new

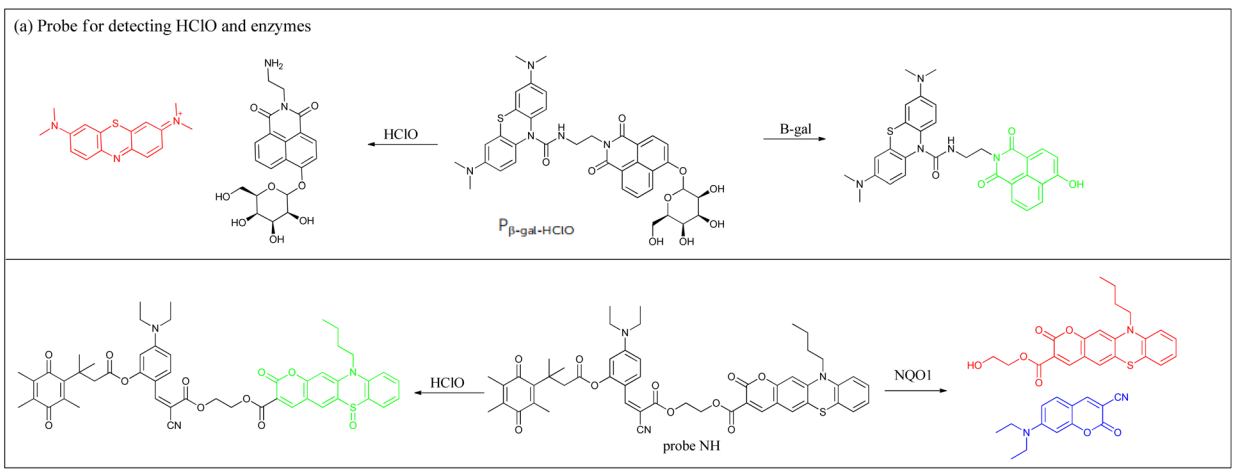

Fig. 9 Molecular structures and sensing mechanism of fluorescent probes. (a) Recognition mechnism of probe for detecting HClO and β-gal or NQO1.

dual-response fluorescent probe (RATP–NClO) for coinstantaneous detection of ATP and ClO^- in complex systems.[79] This RATP–NClO was designed by integrating rhodamine–diethylenetriamine and naphthalimide–thiomorpholine groups (Fig. 10). Upon exposure to ClO^-, the naphthalimide–thiomorpholine group in the RATP–NClO was specially oxidized, emitting green fluorescence. The amido bond in the rhodamine and ATP formed a stable ATP complex, along with dazzling red fluorescence. Using this RATP–NClO, the ATP and ClO^- fluctuations within the cells were clearly visualized. Further research revealed that ATP depletion occurred in the liver of metabolic dysfunction-associated steatohepatitis mice, while the ClO^- content increased simultaneously. Ultimately, the RATP–NClO could be regarded as a double-emission fluorescent probe for monitoring ATP and ClO^- levels in liver diseases.

Wang's group developed dual-channel fluorescent probes (RhTNMB and RhFNMB).[80] The probes linked rhodamine B with methylene blue through diethylenetriamine and triethylenetetramine. These probes themselves did not emit intense fluorescence. After reacting with ATP, the helical structure of the rhodamine B was availably opened, thereby enhancing the red fluorescence. After reacting with HClO, the methylene blue was directly released, showing a significant red fluorescence. Upon exposure to ATP and HClO, the emission peaks of the probe differed by 102 nm at diverse excitation wavelengths, enabling their simultaneous detection. The RhFNMB precisely accumulated in mitochondria, successfully achieving the detection of ATP and HClO in cells (Fig. 11). Through *in vivo* imaging experiments, it was proved that peritonitis caused by *Pseudomonas aeruginosa* generated an increase in ATP and HClO levels, and the therapeutic effect of imipenem was also demonstrated. Furthermore, the ATP and HClO concentrations in the joints of patients with rheumatoid arthritis were significantly higher than those in normal joints. Methotrexate displayed a good therapeutic effect on rheumatoid arthritis. In short, this study will provide a reliable approach for exploring the association between ATP/HClO and rheumatoid arthritis, and offering crucial information for clinical diagnosis and treatment.

Researchers fabricated dual-functional molecular probe (1) for distinguishing ClO^- and ATP in biological systems.[81] The structure was composed of two parts, aminoethylpiperazine linked to rhodamine B and methylene blue. The probe itself was non-fluorescent. After treatment with ClO^-, probe 1 was decomposed into rhodamine B with aminoethylpiperazine and methylene blue, along with a conspicuous emission at 685 nm. Similarly, after reaction with ATP, the lactam ring of probe 1 was quickly opened, emitting yellow fluorescence at 590 nm. Under the stimulation of various inhibitors, stimulants, and acetaminophen (APAP), which was correlated with drug-induced liver injury, probe 1 enabled direct monitoring of intracellular ClO^- and ATP levels. This probe 1 was used to observe the overexpression of ClO^- levels and low concentrations of ATP in APAP-simulated hepatotoxicity. This study developed a reliable way of evaluating the interaction between ATP and ClO^- under experimental conditions.

A fluorescent probe (A-H) was successfully synthesized for divisionally monitoring ATP and HClO.[82] The methylene blue and rhodamine 6G were successfully connected through a linker, thereby establishing recognition sites for the sensing of ATP and HClO. Probe A-H exhibited differentiable fluorescence peaks for HClO and ATP in *in vitro* testing systems. The intracellular confocal imaging results confirmed that A-H effectively monitored HClO and ATP levels within the cancer cells. The A-H interacted with the excessive HClO, and then released MB, carrying out photodynamic therapy.

The structures of these reported fluorescent probes are very similar. In the design, these reported fluorescent probes adopted the strategy of complexing with ATP. *In vitro* tests proved that these probes were capable of synchronously monitoring

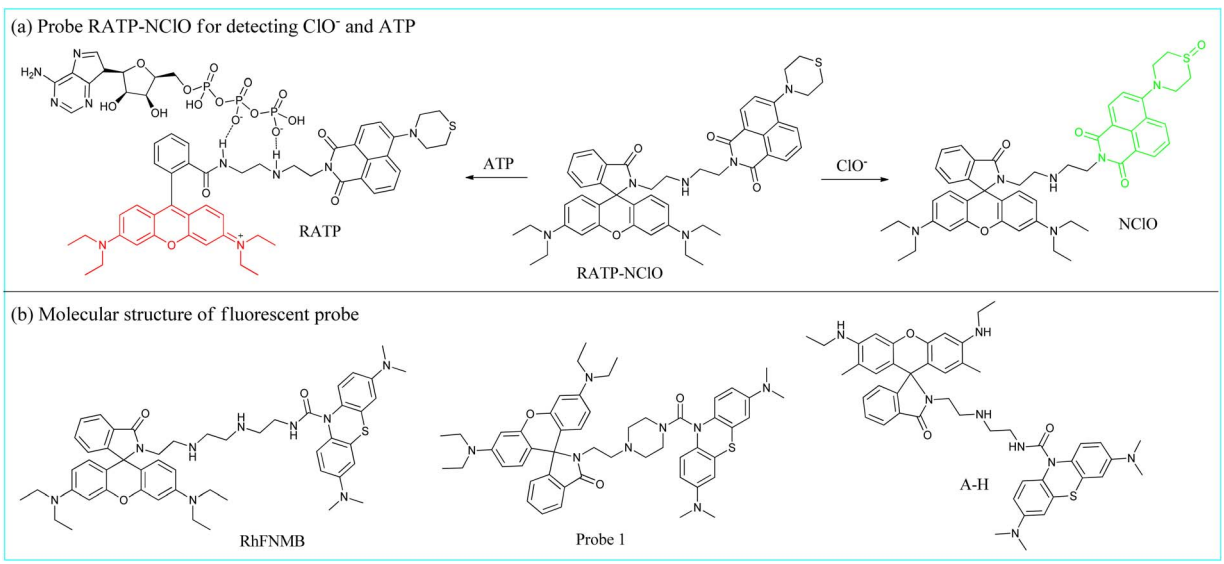

Fig. 10 (a) Sensing mechanism of RATP–NClO and (b) molecular structures of fluorescent probes.

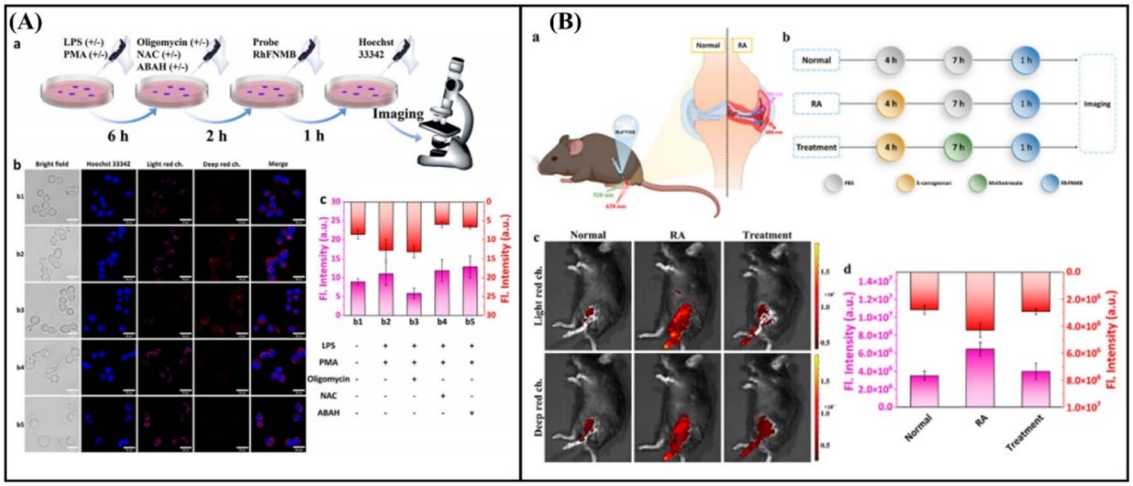

Fig. 11 Fluorescence imaging of the probe RhFNMB in cells (A) and RA mice (B). This figure has been reproduced from ref. 80 with permission from American Chemical Society, copyright 2024.

ATP and ClO^- in the presence of other species. Moreover, the ATP and ClO^- fluctuations were simultaneously detected under different conditions with the help of fluorescence confocal microscopy and these probes. These findings highlighted the potential applications of monitoring the metabolic dysfunction-associated steatohepatitis pathogenic mechanism.

2.6 Detecting HClO/ClO^- and metal ions

Metal ions play an indispensable role in key fundamental biological processes, including signal transmission and managing cellular energy. Among the numerous metal ions, zinc(II) (Zn^{2+}), copper(II) (Cu^{2+}) and ferric ions (Fe^{3+}) engage in different amounts of physiological activity. For example, Zn^{2+} ions are the second most common transition metal ions. They regulate the activity of numerous proteins that are crucial for cognitive

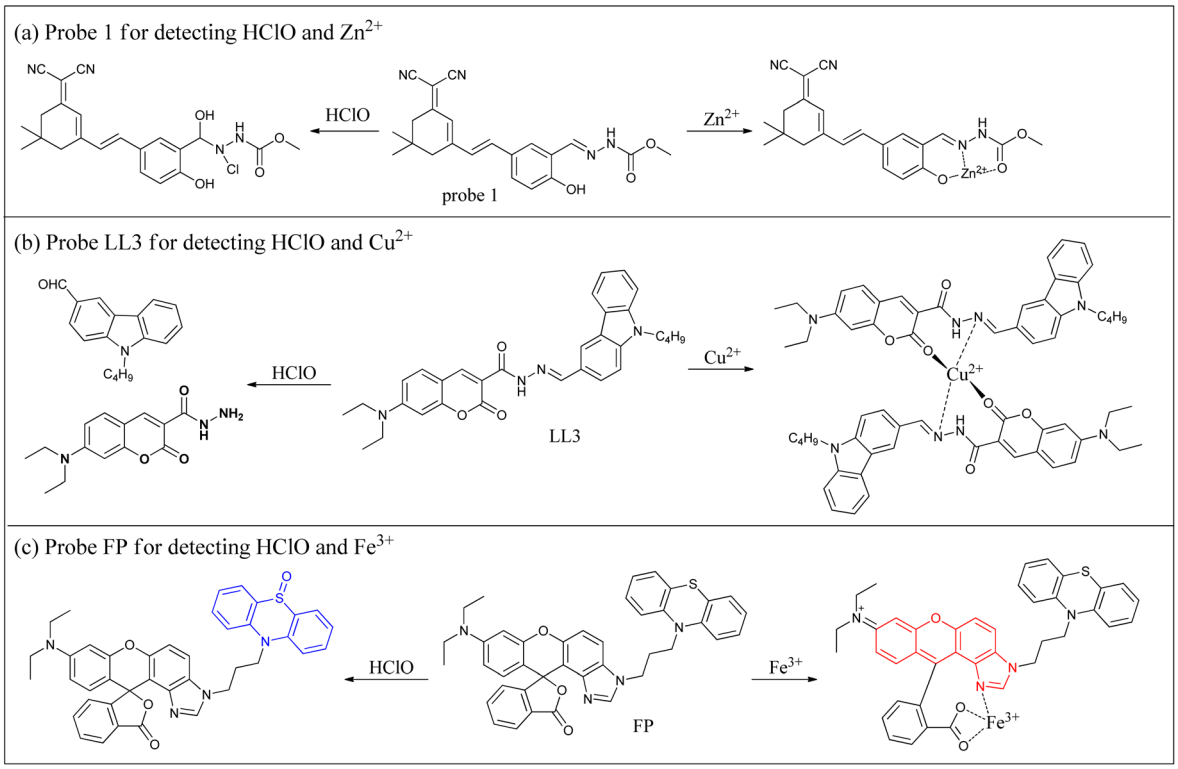

Fig. 12 Sensing mechanism and molecular structures of fluorescent probes. (a) Probe 1 for detecting HClO and Zn^{2+}. (b) Probe LL3 for detecting HClO and Cu^{2+}. (c) Probe FP for detecting HClO and Fe^{3+}.

biological functions and the integrity of the immune system. Cu^{2+} is an important cofactor for enzymes, and acts as a signaling molecule in multiple signal pathways. Monitoring the changes of these metal ions and HClO is of great value for revealing intracellular signaling pathways, metabolic regulation, and disease mechanisms. In view of these important characteristics, Yan's group cleverly created a novel fluorescent probe (1) for distinguishing the detection of Zn^{2+} and HClO (Fig. 12). To gain a targetable biosensor, a dicyanoisophorone derivative and methyl hydrazate were assembled into the entire structure.[83] Upon binding with Zn^{2+} and methyl hydrazate by a Schiff base moiety, an illustrious emission was exhibited at 653 nm. Additionally, in the presence of HClO, fluorescence of reactive solutions shifted from 670 nm to 705 nm. Soon afterwards, the Zn^{2+} and HClO variations in cells were visually imaged with the assistance of a biosensor and fluorescence confocal instrument.

Utilizing the hydrazone derivative, Zhu's team designed a dual-responsive fluorescent probe (LL3) for sensing Cu^{2+} and ClO^-.[84] In the identification process, probe LL3 and Cu^{2+} formed a 2 : 1 complex, accompanied by changes in the solution's color. Upon responding with ClO^-, an imine bond was discerned and hydrolyzed to carbazole aldehyde. By utilizing these two identification mechanisms, the probe LL3 was capable of detecting Cu^{2+} and ClO^-. Moreover, probe LL3 was triumphantly applied for the detection of intracellular Cu^{2+} and ClO^-. Notably, the LL3 enabled the detection of Cu^{2+} in test strips and real water samples.

Huang's group utilized a hybrid of fluoran and phenothiazine to prepare a dual reaction probe (FP) for detecting Fe^{3+} and ClO^-.[85] In the buffer solutions, Fe^{3+}-promoted spiro-lactone ring opening of fluoran, along with strong fluorescence signals at 582 nm. After interacting with HClO, phenothiazine was oxidized and produced a fluorescent product at 376 nm. The distance between these two fluorescence peaks was 206 nm, which was used to distinguish and detect Fe^{3+} and ClO^-. Regrettably, the probe FP was used for monitoring Fe^{3+} in HeLa cells.

These studies provided direct evidence for the changes between HClO/ClO^- and metal ions. Regrettably, the emission wavelengths of the reported probes were mainly concentrated in the short-wave or visible range. Furthermore, these probes are used for imaging studies of HClO/ClO^- and metal ions within cells. In the future, efforts can be focused on developing NIR probes to facilitate detection within deep tissues.

2.7 Detecting HClO/ClO^- and other species

Apart from the reactive species, there are other species present within the organism. For instance, researchers developed a molecular fluorescent probe (dfBDP) utilizing BODIPY dye.[86] The *p-tert*-butyldimethylsilanolate benzyl thioether simultaneously served as a detection site for F^- and HClO in the probe structure (Fig. 13). Through different reaction mechanisms, two differentiable fluorescence peaks were generated in reaction solutions containing dfBDP and F^- or HClO, realizing the simultaneous detection of F^- and HClO (Fig. 14). Furthermore, the dfBDP exhibited high specificity and sensitivity toward F^- and HClO. The confocal fluorescence imaging results indicated that there was a straightforward correlation between the oxidative stress caused by F^- and the upregulation of HClO. Most importantly, this dfBDP was resoundingly used for determining F^- and HClO content in mice. As an effective method, this dfBDP exhibited great application prospects for detecting F^- and HClO under different oxidative stress.

Wang's group synthesized a dual-response fluorescent probe (NS) for distinguishing between HClO and hydrazine (N_2H_4).[87] The NS displayed several merits toward the analytes (HClO and N_2H_4), such as different emission wavelengths of HClO at 548 nm and N_2H_4 at 448 nm, lower detection limit for HClO (11.4 nM) and N_2H_4 (48 nM) and so on. Considering its outstanding characteristics, the NS was employed to detect HClO and N_2H_4 in food samples, plants, and living cells. Wang's group also designed a new molecular fluorescent probe (PTZ-BA) for the recognition of HClO and N_2H_4 in living systems.[88] Disappointingly, after reacting with HClO and N_2H_4, the emission wavelengths of the reacting solutions were relatively close and spectral overlaps easily occurred.

Hu used a phenothiazine and quinoline derivative to design and construct a kind of molecular probe (PTMQ) *via* a C=C double bond,[89] which distinguished detection of N_2H_4 and ClO^- in the presence of numerous reactive molecules. Astoundingly, the N_2H_4 had the ability to break the double bond, and then generated a fluorescent product. *In vitro* experiments demonstrated that the probe PTMQ displayed superiority toward N_2H_4

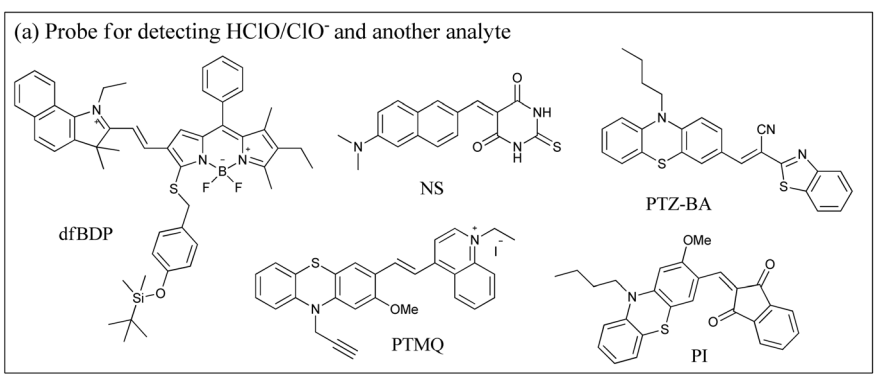

Fig. 13 Molecular structures of fluorescent probes. (a) Probe for detecting HClO/ClO^- and another analyte.

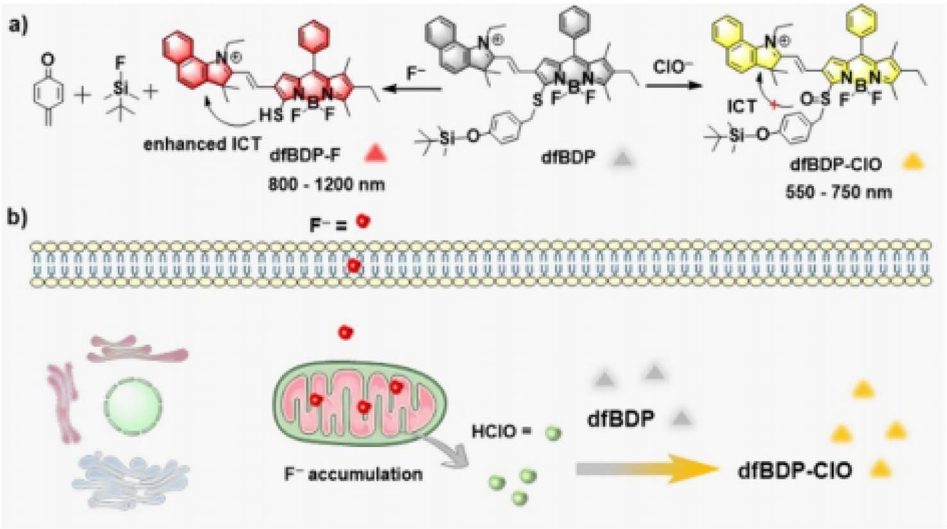

Fig. 14 (a) The recognition mechanism and (b) intracellular application of probe dfBDP. This figure has been reproduced from ref. 86 with permission from American Chemical Society, copyright 2024.

and ClO^-, such as fast response. Owing to its good biocompatibility, it was used for detecting intracellular dual-analytes (N_2H_4 and ClO^-). Utilizing the same identification mechanism, Xia's team synthesized a novel fluorescent probe (PI) by replacing a quinoline derivative with 1,3-indanedione.[90] Subsequently, the PI was applied for N_2H_4 and ClO^- fluxes in cells, zebrafish, and *Arabidopsis thaliana*.

These studies have fully demonstrated the fluctuation patterns of HClO/ClO^- and other reactive molecules under certain complex conditions. Of course, HClO/ClO^- also participated in many unknown venues and signaling pathways. Therefore, more dual-channel probes of HClO/ClO^- and other species need to be constructed to reveal the underlying mechanisms.

2.8 Detecting HClO/ClO^- and the microenvironment

The normal functioning of life activities requires the common regulation by many species and the microenvironment. In other words, intracellular species fluctuations are often accompanied by changes in the microenvironment. Various physical parameters in the cellular microenvironment, such as pH, viscosity, and polarity, continuously influence the occurrence and development of biochemical reactions within the cells. For instance, Lv's group created a novel fluorescent probe (Lyso-VH) with

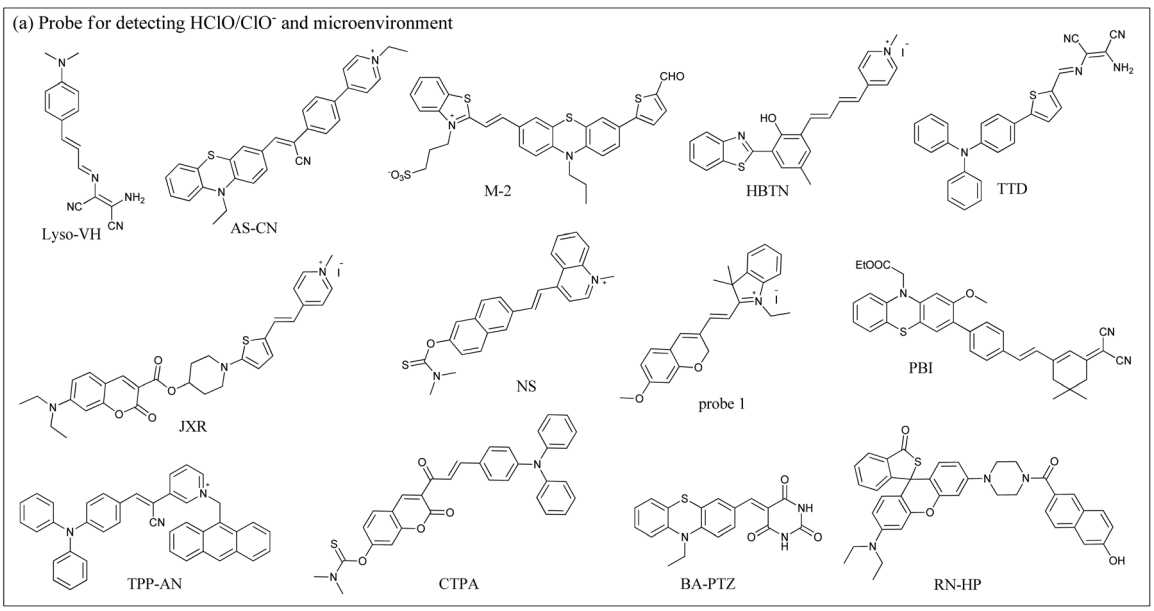

Fig. 15 Molecular structures of fluorescent probes. (a) Probe for detecting HClO/ClO^- and microenvironment.

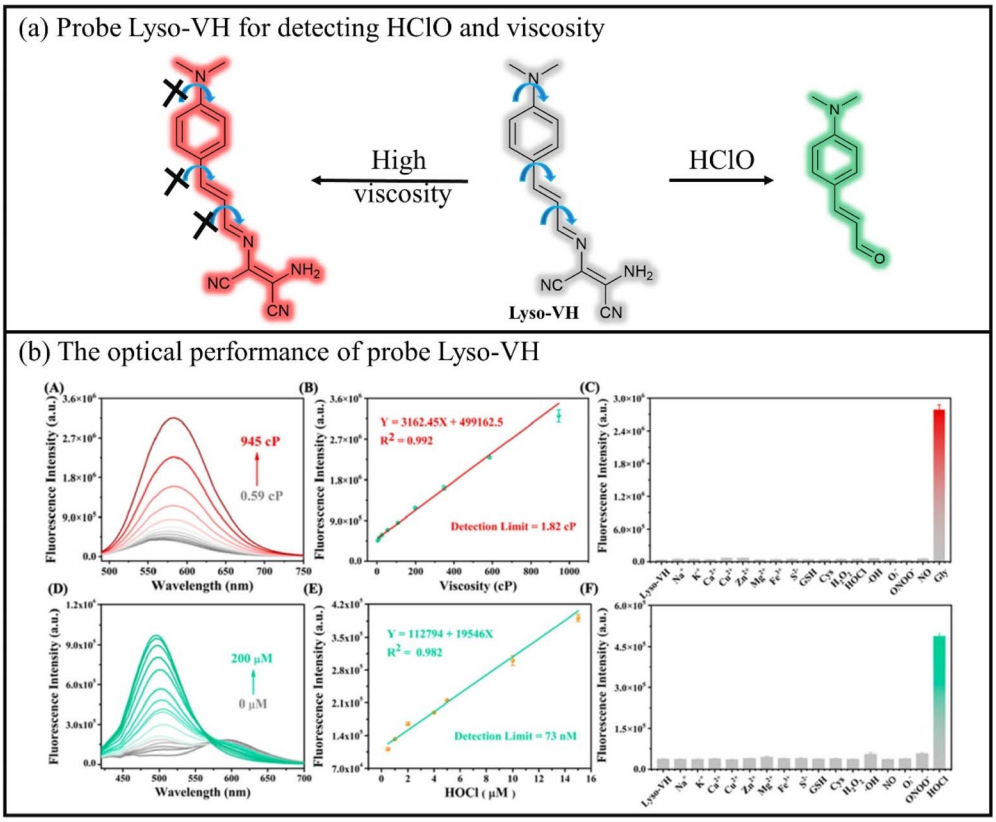

Fig. 16 (a) The recognition mechanism and (b) optical performance of probe Lyso-VH. This figure has been reproduced from ref. 91 with permission from American Chemical Society, copyright 2022.

dual-response characteristics (Fig. 15), which simultaneously detected viscosity and HClO *via* distinguishable emission wavelengths.[91] As the environmental viscosity increased, the red fluorescence of the Lyso-VH was restrained because the single bond in the molecule rotated freely (Fig. 16). Additionally, when HClO oxidized the C–N bond, a new product with typical ICT configuration was generated. The cell co-localization experiments indicated that Lyso-VH mainly gathered into lysosomes. Moreover, Lyso-VH was employed to study HClO and viscosity variations in living cells. Therefore, this work provided a potent sensor that measured the fluctuations of lysosomal HClO and viscosity in the process of acute lung injury.

Yu's group proposed a new NIR fluorescent probe (AS-CN) with a representative D–π–A structure, which simultaneously measured HClO and viscosity.[92] The remarkable fluorescence emission of AS-CN focused on 710 nm in high-viscosity solvents. Moreover, the fluorescence intensity steadily strengthened with the increase in environmental viscosity. Meanwhile, HClO possessed the ability to enhance the fluorescence at 593 nm. Furthermore, the AS-CN exhibited many excellent properties. The authors successfully conducted the study on the synchronous variations of HClO and viscosity in the formation of foam cells. Additionally, the researchers applied AS-CN to conduct non-invasive diagnosis of atherosclerotic mice, and then performed the assessment of atherosclerosis.

Zhang's group reported three fluorescent probes (M1, M2 and M3), which aimed at simultaneously detecting mitochondrial HClO and viscosity.[93] Compared to other probes, M2 exhibited good detection performance, such as high sensitivity. The co-localization experiments demonstrated that the probe M2 could accurately target into mitochondria and simultaneously image the changes in HClO and viscosity. Using this probe, the higher HClO concentrations and viscosity in the atherosclerotic mice were clearly visualized, enabling the distinction between normal and atherosclerotic conditions. Therefore, this probe will be helpful for the early diagnosis of atherosclerotic diseases.

Wang's team developed a difunctional mitochondrial-targetable fluorescent probe (HBTN) for visualizing viscosity and HClO influxes.[94] At different emission wavelengths, HBTN detected viscosity and HClO in the buffer solution. Notably, HBTN was used for monitoring the mitochondrial viscosity, as well as exogenous and endogenous HClO fluctuations. Moreover, employing this HBTN, the viscosity and HClO variations in zebrafish were clearly observed. The excellent performance of HBTN convinced researchers that it was a molecular sensor for detecting viscosity and HClO in diverse disease models.

A new fluorescent probe (TTD) based on triphenylamine–thiophene was constructed by Shuang's group for the simultaneous monitoring of viscosity and ClO^- content.[95] In a high-viscosity environment, the rotation of intramolecular single

bond in the probe was hindered, thereby activating the red fluorescence wavelength at 600 nm. Meanwhile, due to the existence of ClO^-, the imino group underwent an oxidation reaction with aldehyde to form a product, which resulted in a significant fluorescence signal at 460 nm. Subsequently, using this tool, the intracellular viscosity and HClO fluctuations were severally visualized under dual-channel wavelengths.

Using the FRET/TICT mechanism, Yan's team skillfully designed a novel molecular fluorescent probe (JXR) that simultaneously detected HClO and viscosity at different emission wavelengths.[96] As HClO concentrations continuously increased, a gradually decreasing red signal at 594 nm and a continuously increasing blue signal at 470 nm were clearly observed. Furthermore, the increasing environmental viscosity effectively inhibited the intramolecular rotation, and the red signals at 594 nm increasingly rose, enabling the detection of viscosity. Importantly, the JXR enabled the study of HClO and viscosity in cells and zebrafish.

Yu's group introduced a dual-response mitochondrial-targeted fluorescent probe (NS), which was applied to monitor HClO and viscosity in atherosclerosis-related foam cells.[97] A rotatable linker was regarded as the activation group for viscosity. When environmental viscosity increased, the NS exhibited a linear fluorescence enhancement. However, after activation with HClO, reactive solutions presented evident fluorescence variations, achieving ratiometric fluorescence measurement of HClO. Due to its mitochondrial targeting ability, the NS achieved *in situ* monitoring of mitochondrial viscosity and HClO variations in RAW 264.7 cells. Notably, the NS achieved synchronous detection of mitochondrial viscosity and HClO in macrophage-derived foam cells, uncovering a precise correlation between the HClO levels and mitochondrial viscosity in the process of atherosclerosis. This work offered a new strategy for imaging mitochondrial viscosity and HClO in the early diagnosis of atherosclerosis.

Employing this chromene-hemicyanine dye, Xu's team created a novel fluorescent probe (1) for dual-channel detection of ClO^- and viscosity.[98] As the environmental viscosity of the solution increases, the NIR fluorescence at 628 nm gradually enhanced, because the rotation of the single bonds in the molecule was availably restricted. Importantly, the increase in fluorescence showed a good positive correlation with environmental viscosity. In addition, the C=C double bond was specifically interrupted in the presence of other reactive species, and then generated a fluorescent product at 493 nm. Probe 1 accurately accumulated in the mitochondria. Subsequently, the ClO^- and viscosity in living C6 cells and zebrafish were consecutively bioimaged with the help of probe 1 and a confocal fluorescence instrument.

Tian's team utilized phenothiazine and C=C double bonds as sensing moieties of ClO^- and viscosity to fabricate a molecular probe (PBI).[99] The probe PBI displayed several attractive characteristics for ClO^- and viscosity in *in vitro* experiments, mainly large Stokes shift (177 nm) visual detection. Soon afterwards, PBI was applied for visual detection of their variations in zebrafish.

To monitor mitochondrial ClO^- and viscosity, Huang's group employed a positive pyridinium to prepare a novel fluorescent probe (TPP-AN).[100] When the concentrations of ClO^- or the environmental viscosity was changed, the reaction solution emitted fluorescence of different wavelengths, enabling their distinction and detection. Taking advantage of this advantage, mitochondrial ClO^- variations were directly visualized.

Yan's group developed a new dual-channel fluorescent probe (CTPA) for imaging HClO and polarity. In the probe's structure, *N*,*N*-dimethylthiocarbamate and 7-hydroxycoumarin were selected as the sensing moiety and fluorophore.[101] Among them, the introduction of triphenylamine into the probe design was conducive to monitoring polarity fluctuations. The satisfactory characters of the CTPA enabled its successful application in detecting endogenous and exogenous ClO^- and polarity. It was able to distinguish HeLa cells from HIN-3T3 cells through ClO^- and polarity. In the end, this work provided an excellent approach for the preparation of dual-responsive probes.

To detect the changes of HClO and polarity within the lipid droplets, Ye's group designed a bifunctional fluorescent probe (BA-PTZ).[102] As the environmental polarity decreased, the fluorescence of the BA-PTZ steeply intensified, facilitating the detection of polarity. As the concentration of HClO increased, the C=C double bond and S atom both were oxidized and generated a new product, along with strong fluorescence, enabling detection of HClO. Since the probe BA-PTZ was a lipophilic compound, it was very likely to accumulate within the lipid droplets. Due to its outstanding detection capability, the HClO and polarity fluctuations were simultaneously monitored in ferroptosis cells.

Zheng's group introduced a new fluorescent probe (RN-HP), which concurrently visualized HClO and pH through independent emission channels.[103] This RN-HP used rhodamine and naphthalene as the fluorophores for detecting HClO and environmental pH fluctuations. After reaction with HClO, the emission signals of RN-HP significantly increased at 577 nm, demonstrating excellent selectivity and high sensitivity. However, the fluorescence signals at 460 nm varied with pH changes. As could be seen from the fluorescence spectra, the two fluorescence peaks differed by 117 nm, effectively avoiding interference and spectral overlap. This RN-HP had capability of the analysis of HClO and pH values in cells and actual samples. Therefore, in this work, a reliable tool was prepared for studying the interaction of the microenvironment.

These studies not only served as some powerful tools for visualizing the fluctuations of HClO and the microenvironment (viscosity, polarity, pH) in organelles, cells and so on, but also offered new insights into symptoms and diseases. Moreover, all of this evidence strongly indicated that the changes in reactive molecules were closely related to the microenvironment. In other words, changes in the microenvironment often triggered alterations in reactive molecules. Finally, these tools not only performed well in conventional cell experiments, but also demonstrated feasibility in the dynamic monitoring of foam cell formation in both channels. The successful development of these detection tools contributed to the elucidation of the

underlying functions of HClO/ClO^- and the microenvironment in certain diseases, such as atherosclerosis.

3. Conclusion

In this review, we summarized the design concepts, spectral characteristics and biological applications of dual-detection small-molecule fluorescent probes that were used for the simultaneous determination of HClO/ClO^- and analytes ($ONOO^-$, H_2O_2, $^{\cdot}OH$, SO_2, Cys, ATP, NQO1, β-gal)/microenvironment (viscosity, polarity, pH) in recent years. Moreover, the reported dual-response fluorescent probes successfully achieved the visualization and monitoring of the HClO/ClO^- and analytes/microenvironment in various physiological processes and diseases, including neurodegenerative diseases, cancer, inflammatory conditions, liver injury, *etc.* Compared with the one species-responsive fluorescent probes, double species-responsive fluorescent probes could facilitate a more comprehensive study of their concentrations and pathological mechanism between HClO/ClO^- and analytes. Overall, the fluorescent probes for simultaneously detecting HClO/ClO^- and analytes/microenvironment were ideal tools for tracking living cells and the progression of diseases in animals, opening up new perspectives for a better understanding of some diseases. For instance, Wang's group created a novel probe (MB-NAP) for monitoring HClO and Cys variations in AKI mice. MB-NAP was proven to possess outstanding performance in drug screening. It achieved real-time monitoring of HClO and Cys. Additionally, Lv's group masterfully prepared a molecular sensor (Lyso-VH) for simultaneous monitoring of HClO and viscosity in drug-induced pyroptosis. The development and utilization of these tools had greatly facilitated the relationships between reactive species and the microenvironment, thereby contributing to the elucidation of pathological mechanisms in certain diseases.

Although significant progress has been made in the preparation of double-site fluorescent probes for severally detecting HClO/ClO^- and analytes/microenvironment, there are still some issues that need to be addressed. Firstly, many of the fluorescent probes mentioned for detecting HClO/ClO^- and analytes/microenvironment still suffer from short emitting wavelengths, mainly focusing on the visible light spectral range and NIR-I region. That is to say, the currently developed dual response fluorescent probes are rarely used in the NIR-II region (1000–1700 nm), while this region displays significant advantages for deep tissue *in vivo*, presenting high signal-to-noise ratio imaging and deep tissue penetration. Secondly, probes can provide more accurate information *via* combining with multimodal imaging techniques (photoacoustic imaging, fluorescence lifetime imaging). Thirdly, by using these dual-response fluorescent probes to detect HClO/ClO^- and analytes/microenvironment, significant achievements are expected in exploring various physiological and pathological mechanisms. This will provide new insights for biological research in the fields of drug discovery and fluorescent imaging. Fourthly, apart from its roles in mitochondria, the function of HClO/ClO^- and analytes/microenvironment in other organelles (such as the endoplasmic reticulum and the Golgi apparatus) still requires further investigation. Fifthly, the low selectivity of the sensing group may lead to interference from several substances. For example, the benzoboric acid ester moiety was widely used for the detection of H_2O_2. However, this moiety was also employed for the identification of $ONOO^-$. Improving the specificity of the recognition unit, or developing outstanding single-molecule fluorescent probes capable of monitoring multiple indicators simultaneously, will play a crucial role in other types of life processes. Sixthly, to establish a precise relationship between the levels of reactive molecules and damage degree, we can develop some ratiometric-type fluorescent probes, offering a new perspective for investigating the pathogenic mechanism. Finally, the principle of deep penetration of long-wavelength light and sound waves should be utilized to construct a variety of dual-mode probes for near-infrared region II (NIR II) fluorescent and photoacoustic imaging. These probes combine the high sensitivity of fluorescence imaging with the deep imaging capability of photoacoustic imaging, which is conducive to achieving more in-depth and more sensitive *in vivo* diagnosis, and are expected to provide new opinions for early lesions. In short, we hope this review will assist researchers in developing new design strategies and further understanding the fundamental roles and cooperation mechanism of HClO/ClO^- and analytes/microenvironment in certain diseases.

Author contributions

Yongqing Zhou: conceptualization, investigation, writing – original draft (lead), review and editing, funding acquisition. Mei Yan: review and editing. Hosoowi Lee: review and editing, funding acquisition. Juyoung Yoon: conceptualization, review and editing, supervision and funding acquisition.

Conflicts of interest

The authors declare that they have no known competing financial interests or personal relationships that could have appeared to influence the work reported in this paper.

Data availability

No primary research results, software or code have been included and no new data were generated or analyzed as part of this review.

Acknowledgements

This work was financially supported by the National Natural Science Foundation of China (22207038) and the Natural Science Foundation of Shandong Province (ZR2024QB027). J. Y. thanks the National Research Foundation of Korea for the grant funded by the Korean government (MSIT) (2022R1A2C3005420). H. L. is thankful for the National Research Foundation of Korea (NRF) grant funded by the Korea government (MSIT) (RS-2024-00345550).

References

1 S. Debnath, R. Ghosh, R. R. Nair, D. Pradhan and P. B. Chatterjee, *ACS Omega*, 2022, **7**, 38122–38149.
2 J. Leopold and J. Schiller, *Antioxidants*, 2024, **13**, 921.
3 M. Winter, D. Boecker and W. Posch, *Viruses*, 2025, **17**, 1219.
4 W. Chen, C. Zhang, J. Wang, M. Jiang, J. Sheng, K. Li, X. Dong, L. Yang and S. Zhang, *Anal. Chem.*, 2025, **97**, 17521–17528.
5 S. Li, M. Deng, Y. Liu, Y. Luo, H. Zhang, P. Wang, Z. Zhai, D. Cheng and L. He, *Anal. Chem.*, 2025, **97**, 17857–17864.
6 Y. Cao, J. Gu, Z. Chen, J. Gao, J. Yang, W. Wu, M. Fang, Q. Li, B. Liu and Z. Li, *Adv. Mater.*, 2025, **37**, 2408941.
7 H. Liu, R. Lv, F. Song, Y. Yang, F. Zhang, L. Xin, P. Zhang, Q. Zhang and C. Ding, *Chem. Sci.*, 2024, **15**, 5681–5693.
8 B. Gu, C. Dai, Z. Zhou, S. Tang and Y. Zhang, *Sens. Actuators, B*, 2023, **375**, 132900.
9 X. He, Z. Zheng, F. Zhang, C. Xu, W. Xu, L. Ye, X. Sun, Z. Zhou and J. Shen, *ACS Appl. Bio Mater.*, 2020, **3**, 7886–7897.
10 T. Yang, Y. Fang, Q. Zhang, F. Wang, X. Xu and C. Li, *Sens. Actuators, B*, 2024, **417**, 136138.
11 X. Wang, Q. Ding, R. R. Groleau, L. Wu, Y. Mao, F. Che, O. Kotova, E. M. Scanlan, S. E. Lewis, P. Li, B. Tang, T. D. James and T. Gunnlaugsson, *Chem. Rev.*, 2024, **124**, 7106–7164.
12 J. Ma, R. Sun, K. Xia, Q. Xia, Y. Liu and X. Zhang, *Chem. Rev.*, 2024, **124**, 1738–1861.
13 X. Li, X. Gao, W. Shi and H. Ma, *Chem. Rev.*, 2014, **114**, 590–659.
14 V.-N. Nguyen, J. Ha, M. Cho, H. Li, K. M. K. Swamy and J. Yoon, *Coord. Chem. Rev.*, 2021, **439**, 213936.
15 J. Yan, S. Lee, A. Zhang and J. Yoon, *Chem. Soc. Rev.*, 2018, **47**, 6900–6916.
16 Y.-X. Ye, J.-C. Pan, H.-C. Wang, X.-T. Zhang, H.-L. Zhu and X.-H. Liu, *Chem. Soc. Rev.*, 2024, **53**, 9133–9189.
17 N. Kwon, D. Kim, K. M. K. Swamy and J. Yoon, *Coord. Chem. Rev.*, 2021, **427**, 213581.
18 M. Cho, V.-N. Nguyen and J. Yoon, *ACS Meas. Sci. Au*, 2022, **2**, 219–223.
19 N. Kwon, Y. Chen, X. Chen, M. H. Kim and J. Yoon, *Dyes Pigm.*, 2022, **200**, 110132.
20 D. Cheng, Y. Pan, L. Wang, Z. Zeng, L. Yuan, X. Zhang and Y.-T. Chang, *J. Am. Chem. Soc.*, 2017, **139**, 285–292.
21 D. Wu, L. Chen, Q. Xu, X. Chen and J. Yoon, *Acc. Chem. Res.*, 2019, **52**, 2158–2168.
22 J.-T. Hou, N. Kwon, S. Wang, B. Wang, X. He, J. Yoon and J. Shen, *Coord. Chem. Rev.*, 2022, **450**, 214232.
23 J. J. Hu, S. Ye and D. Yang, *Isr. J. Chem.*, 2017, **57**, 251–258.
24 Y.-R. Zhang, Y. Liu, X. Feng and B.-X. Zhao, *Sens. Actuators, B*, 2017, **240**, 18–36.
25 M. Ren, K. Zhou, L. He and W. Lin, *J. Mater. Chem. B*, 2018, **6**, 1716–1733.
26 M. K. Goshisht, N. Tripathi, G. K. Patra and M. Chaskar, *Chem. Sci.*, 2023, **14**, 5842–5871.
27 Y. Wen, F. Huo and C. Yin, *Chin. Chem. Lett.*, 2019, **30**, 1834–1842.
28 Y. Zhou, B. Huang, J. Li, M. Yan, C. Wu, C. Cho and J. Yoon, *Anal. Chem.*, 2026, **98**, 214–223.
29 Z. Cheng, S. Benson, L. Mendive-Tapia, E. Nestoros, C. Lochenie, D. Seah, K. Y. Chang, Y. Feng and M. Vendrell, *Angew. Chem., Int. Ed.*, 2024, **63**, e202404587.
30 L. Zhang, L. Zhang, X. Zhang, Y. Zhao, S. Fang, J. You and L. Chen, *Trends Anal. Chem.*, 2023, **169**, 117377.
31 Q. Xu, K.-A. Lee, S. Lee, K. M. Lee, W.-J. Lee and J. Yoon, *J. Am. Chem. Soc.*, 2013, **135**, 9944–9949.
32 C. Ma, S. Hou, X. Zhou, Z. Wang and J. Yoon, *Anal. Chem.*, 2021, **93**, 9640–9646.
33 N. Yin, Y. Wang, G. Qin, M. Wang, J. Tang, X. Yao, Q. Xu and J. Yoon, *Sens. Actuators, B*, 2024, **419**, 136419.
34 X. Chen, K.-A. Lee, X. Ren, J.-C. Ryu, G. Kim, J.-. Ryu, W.-J. Lee and J. Yoon, *Nat. Protoc.*, 2016, **11**, 1219–1228.
35 M. M. Fortibui, S. A. Yoon, S. Y. Yoo, J. Y. Son and M. H. Lee, *Coord. Chem. Rev.*, 2024, **510**, 215800.
36 M. Li, P. Lei, S. Shuang, C. Dong and L. Zhang, *Spectrochim. Acta, Part A*, 2023, **303**, 123179.
37 J. He, X. Han and Y. Yue, *Analyst*, 2025, **150**, 3045–3070.
38 Z. Li, C. Peng, Q. Liu, Y. Du, J. Zhang, Y. Li and H. Yu, *Anal. Chem.*, 2025, **97**, 22071–22080.
39 Q. Zan, L. Fan, R. Wang, H. Wang, Y. Huang, X. Yu, Y. Zhang, C. Dong and S. Shuang, *Biosens. Bioelectron.*, 2025, **282**, 117495.
40 Y. Xu, F. Nian, J. Wei, L. Li, R. Ma, S. Ma and W. Wang, *Chem. Commun.*, 2025, **61**, 13409–13412.
41 Z. Wu, B. Yang, Z. Lu, Y. Li, Y. Li, J. Wang, R. Yao, J. Zeng, Z. Geng and Z. Wang, *Anal. Chem.*, 2025, **97**, 22132–22144.
42 M. Yang, Z. Kang, X. Zhong, S. Bai, D.-E. Wang, Q. Tu, S. Chen, J. Wang and M.-S. Yuan, *Adv. Healthcare Mater.*, 2025, **14**, 2500907.
43 X. Zhou, Y. Luo, S. Jin, T. Xu, Y. Liang, Z. Meng, X. Xu, S. Wang and Z. Wang, *Anal. Chem.*, 2025, **97**, 21558–21571.
44 J. Liu, W. Zhang, X. Wang, Q. Ding, C. Wu, W. Zhang, L. Wu, T. D. James, P. Li and B. Tang, *J. Am. Chem. Soc.*, 2023, **145**, 19662–19675.
45 T. Huang, S. Yan, Y. Yu, Y. Xue, Y. Yu and C. Han, *Anal. Chem.*, 2022, **94**, 1415–1424.
46 W. Huang, X. Du, C. Zhang, S. Zhang, J. Zhang and X.-F. Yang, *Anal. Chem.*, 2022, **94**, 17485–17493.
47 Y. Zhou, J. Zeng, Q. Yang and L. Zhou, *Spectrochim. Acta, Part A*, 2022, **282**, 121691.
48 J. Tang, S. Deng, Y. Xie, S. Li, Y. Qiao, L. Zhu, J. Guo, J. Zhou and Y. Ye, *Dyes Pigm.*, 2024, **227**, 112183.
49 L.-L. Wang, J.-Y. Bai, X.-F. Li, M.-H. Zheng, Y. Miao and J.-Y. Jin, *Anal. Chim. Acta*, 2021, **1183**, 338980.
50 R. Zhang, J. Zhao, G. Han, Z. Liu, C. Liu, C. Zhang, B. Liu, C. Jiang, R. Liu, T. Zhao, M.-Y. Han and Z. Zhang, *J. Am. Chem. Soc.*, 2016, **138**, 3769–3778.
51 J. Ma, X. Kong, X. Wang, M. Zhao, H. Xie, Z. Jiao and Z. Zhang, *Sens. Actuators, B*, 2024, **417**, 136209.
52 J. Han, X. Liu, H. Xiong, J. Wang, B. Wang, X. Song and W. Wang, *Anal. Chem.*, 2020, **92**, 5134–5142.

53 P. Niu, J. Liu, F. Xu, L. Yang, Y. Li, A. Sun, L. Wei, X. Liu and X. Song, *ACS Appl. Bio Mater.*, 2022, **5**, 1683–1691.
54 Y. Du, B. Wang, D. Jin, M. Li, Y. Li, X. Yan, X. Zhou and L. Chen, *Anal. Chim. Acta*, 2020, **1130**, 174–182.
55 Y. M. Wang, J. Li, J. H. Chen, B. Liu, Y. Zeng, J.-Y. Lim, Y. T. Liu, J. F. Zhang, X. H. Wu and W. X. Ren, *Dyes Pigm.*, 2023, **215**, 111218.
56 Q. He, S. Zang, Y. Zeng, B. Wang and X. Song, *Spectrochim. Acta, Part A*, 2025, **328**, 125464.
57 Z. Zhao, W. Xiang, W. Guo and B. Wang, *Anal. Chem.*, 2025, **97**, 2127–2135.
58 P. Huang, W. Zhang, J. Wang, F. Huo and C. Yin, *Chin. Chem. Lett.*, 2025, **36**, 109778.
59 M. Ren, Z. Li, B. Deng, L. Wang and W. Lin, *Anal. Chem.*, 2019, **91**, 2932–2938.
60 X. Jiao, Y. Xiao, Y. Li, M. Liang, X. Xie, X. Wang and B. Tang, *Anal. Chem.*, 2018, **90**, 7510–7516.
61 X. Yue, J. Wang, J. Han, B. Wang and X. Song, *Chem. Commun.*, 2020, **56**, 2849–2852.
62 W. Cheng, X. Xue, L. Gan, P. Jin, B. Zhang, M. Guo, J. Si, H. Du, H. Chen and J. Fang, *Anal. Chim. Acta*, 2021, **1156**, 338362.
63 S. Chen, X. Liu, Q. Li, S. Fu, H. Zhang, S. Li, L. Wang, C. He, W. Chen and P. Hou, *J. Hazard. Mater.*, 2024, **465**, 133253.
64 Y. Chen, J.-Y. Lim, X. H. Wu, J. S. Heo, F. Yuan, J. F. Zhang, D. W. Yoon and W. X. Ren, *Dyes Pigm.*, 2021, **195**, 109666.
65 N. Ahmed, J. Liu, X. Xu, W. Zareen, Z. Shafiq and Y. Ye, *Dyes Pigm.*, 2024, **224**, 112048.
66 Y. Ai, Z. Zhu, H. Ding, C. Fan, G. Liu and S. Pu, *J. Photochem. Photobiol., A*, 2022, **433**, 114144.
67 Z. Teng, H. Shangguan, L. Liu, S. Zhang, G. Li, Z. Cheng, F. Qi and X. Liu, *Spectrochim. Acta, Part A*, 2024, **316**, 124312.
68 H. Ding, L. Yue, Y. Ai, Z. Zhu, C. Fan, G. Liu and S. Pu, *Spectrochim. Acta, Part A*, 2024, **304**, 123348.
69 J. Yang, S. Tu, T. Feng, T. Wu, W. Zhu, T. Yang, L. Yan, Y. Le and L. Liu, *Microchem. J.*, 2025, **211**, 113160.
70 B. Gu, C. Dai, Z. Zhou, S. Tang and Y. Zhang, *Sens. Actuators, B*, 2023, **375**, 132900.
71 H. Cao, F. Yu, K. Dou, R. Wang, Y. Xing, X. Luo and F. Yu, *Anal. Chem.*, 2024, **96**, 18574–18583.
72 J. Han, S. Yang, B. Wang and X. Song, *Anal. Chem.*, 2021, **93**, 5194–5200.
73 L. Zhang, J. Tan, X. Yang, S. Fang, S. Wei, S. Liu, L. Zhang, X. Wang and L. Chen, *J. Hazard. Mater.*, 2025, **496**, 139543.
74 H. Zhang, L. Hu, Z.-Q. Wang, Z.-Z. Peng, G.-J. Mao, F. Xu, J. Ouyang, L. Hu and C.-Y. Li, *Microchem. J.*, 2024, **205**, 111171.
75 X. Bao, K. Ai, X. Cao, D. Chen, B. Zhou and C. Huo, *Dyes Pigm.*, 2022, **197**, 109928.
76 J. Lan, Y. Wang, Y. Qin, Z. Li, R. Zeng, L. Liu, L. Chen, K. Yang, Y. Ding and T. Zhang, *Dyes Pigm.*, 2022, **207**, 110706.
77 L. Wang, D. Hong, J. Li, L. Wu, Y. Xia, X. Di, J. Wang, Y. Xie, J. Da and Y. Liu, *Chem. Commun.*, 2025, **61**, 5669–5672.
78 X. Yue, Y. Yang, M. Lan, K. Li and B. Wang, *Anal. Chim. Acta*, 2022, **1224**, 340242.
79 M. M. Fortibui, C. Park, N. Y. Kim, T. H. Kim and M. H. Lee, *Anal. Chem.*, 2024, **96**, 9408–9415.
80 W. Qu, R. Tian, B. Yang, T. Guo, Z. Wu, Y. Li, Z. Geng and Z. Wang, *Anal. Chem.*, 2024, **96**, 5428–5436.
81 P.-D. Mao, S.-S. Liu, Z.-Y. Lian, W.-N. Wu, L.-Y. Bian, Y. Wang, Z.-H. Xu and T. D. James, *Sens. Actuators, B*, 2025, **440**, 137908.
82 J. Liu, J. Sun, D. Zhang, X. Yang, Y. Zhao and Y. Ye, *Sens. Actuators, B*, 2025, **429**, 137275.
83 L. Yan, H. Yang, J. Li, C. Zhou, L. Li, X. Wu and C. Lei, *Anal. Chim. Acta*, 2022, **1206**, 339750.
84 L. Liu, C. Guo, Q. Zhang, P. Xu, Y. Cui, W. Zhu, M. Fang and C. Li, *J. Photochem. Photobiol., A*, 2022, **423**, 113593.
85 Q. Wang, D. Zheng, Q. Cao, K. Huang and D. Qin, *Spectrochim. Acta, Part A*, 2021, **261**, 120061.
86 Y. Mei, Z. Hai, Z. Li, K. Rong, W. Tang and Q.-H. Song, *Anal. Chem.*, 2024, **96**, 3802–3809.
87 H. Fang, Z. Qiao, X. Sui, M. Quinto, W. He, W. Zhao and B. Wang, *Spectrochim. Acta, Part A*, 2026, **346**, 126911.
88 Y. Liang, T. Xu, X. Yue, S. Xu, X. Xu, S. Wang and Z. Wang, *J. Hazard. Mater.*, 2025, **488**, 137425.
89 B. Zhu, X. Wu, J. Rodrigues, X. Hu, R. Sheng and G.-M. Bao, *Spectrochim. Acta, Part A*, 2021, **246**, 118953.
90 Y.-Y. Kong, D. Han, X.-Y. Shi, H.-K. Yang, Z. Liu, J.-T. Lin and H.-C. Xia, *J. Mol. Struct.*, 2025, **1321**, 140176.
91 Z. Zhan, Q. Lei, Y. Dai, D. Wang, Q. Yu, Y. Lv and W. Li, *Anal. Chem.*, 2022, **94**, 12144–12151.
92 Z. Wang, S. Wang, B. Wang, J. Shen, L. Zhao, F. Yu and J.-T. Hou, *Chem. Eng. J.*, 2023, **464**, 142687.
93 Q. Cheng, J. Sun, B. Wang, A. Ding, W. Sun, F. Yang and J. Zhang, *Bioorg. Chem.*, 2025, **156**, 108191.
94 W. Qu, B. Yang, T. Guo, R. Tian, S. Qiu, X. Chen, Z. Geng and Z. Wang, *Analyst*, 2023, **148**, 38–46.
95 X. Sun, J. Wang, Z. Shang, H. Wang, Y. Wang and S. Shuang, *J. Mol. Liq.*, 2024, **402**, 124788.
96 X. Zhang, Y. Si, X. Chen, X. Nie, Y. Zhang, L. Lin and Y. Yan, *Molecules*, 2025, **30**, 1531.
97 Y. Cai, H. Hu, Z. Wu and C. Yu, *Spectrochim. Acta, Part A*, 2023, **303**, 123225.
98 S.-L. Xu, F.-F. Guo, Z.-H. Xu, Y. Wang and T. D. James, *Sens. Actuators, B*, 2023, **383**, 133510.
99 S. Shen, Y. Yuan, Y. Wang, Y. Zhu, M. Du, C. Yue, B. Pan, S. Ren, F. Feng and M. Tian, *Spectrochim. Acta, Part A*, 2025, **337**, 126162.
100 X. Huang, T. Luo, C. Zhang, J. Li, Z. Jia, X. Chen, Y. Hu and H. Huang, *Talanta*, 2022, **241**, 123235.
101 M. Li, W. Fang, B. Wang, Y. Du, Y. Hou, L. Chen, S. Cui, Y. Li and X. Yan, *New J. Chem.*, 2021, **45**, 21406–21414.
102 X. Xu, J. Liu, D. Zhang and Y. Ye, *Dyes Pigm.*, 2023, **219**, 111552.
103 J. Zhou, C. Tang, J. Gao, Q. Zhao, X. Wu, Y. Dai, X. Zheng and Z. Zhan, *Spectrochim. Acta, Part A*, 2026, **346**, 126884.